

Master's Thesis

# Gaining Customer Insights with Machine Learning on Graphs

University of Basel  
Faculty of Business and Economics

Degree Program:  
Master of Science (MSc) in Business and Economics

Major:  
Quantitative Methods

Author:  
Michael von Siebenthal

Supervisor:  
Prof. Dr. Dietmar Maringer

Submission Date:  
July 15, 2021

# Abstract

This master's thesis investigates graph machine learning for the purpose of gaining customer insights. Given that customer data is most commonly only available as standard cross-sectional data, semi-synthetic graph generation is investigated. Specifically, it is assessed to what extent semi-synthetic graphs can be utilized for graph machine learning. To assess the viability and competitiveness of this approach, different graph machine learning models are tested. In addition, the graph machine learning results are compared to the results of common standard machine learning models. The findings of the GraphSage model reveal, that using semi-synthetic graphs can indeed be a viable approach. The semi-synthetic graphs can further provide useful results for visualizing relationships within the data. Lastly it is shown, that the semi-synthetic graph could potentially be used for overcoming the difficulties associated with unbalanced label data. Semi-synthetic graphs are shown to be limited by the extent to which they can capture useful graph structures for predicting the label of a given classification task. The uncommon graph properties of semi-synthetic graphs further limit the capabilities of some graph machine learning models. Suggestions for future research is provided and focuses on improving semi-synthetic graph generation, using graphs for cluster analysis, and improving graph machine learning models.

# Table of Contents

<b>Abstract</b>	<b>I</b>
<b>Table of Contents</b>	<b>II</b>
<b>List of Figures</b>	<b>IV</b>
<b>List of Tables</b>	<b>V</b>
<b>List of Algorithms</b>	<b>VI</b>
<b>List of Abbreviations</b>	<b>VII</b>
<b>1 Introduction</b>	<b>1</b>
1.1 General Outline . . . . .	1
1.2 Motivation . . . . .	3
1.3 Machine Learning Overview . . . . .	4
1.4 Research Topic . . . . .	6
<b>2 Theory</b>	<b>8</b>
2.1 Graph Theory . . . . .	8
2.2 Machine Learning on Graphs . . . . .	13
2.2.1 Graph Representation Learning . . . . .	14
2.2.2 Graph Neural Networks . . . . .	18
2.2.2.1 Graph Convolutional Networks . . . . .	21
2.2.2.2 GraphSage . . . . .	23
2.3 Graph Generation . . . . .	26
<b>3 Data</b>	<b>30</b>
3.1 Software & Code . . . . .	31
3.2 Self Launched Survey . . . . .	31
3.3 Bank Telemarketing Dataset . . . . .	32
3.4 US Airline Passenger Dataset . . . . .	35
3.4.1 Graph Generation . . . . .	38
3.4.2 Stochastic vs. Deterministic MAGs . . . . .	44
<b>4 Results</b>	<b>47</b>
4.1 Graph Representation Learning . . . . .	47
4.2 Graph Neural Networks . . . . .	49
4.2.1 Graph Convolutional Networks . . . . .	50
4.2.2 GraphSage . . . . .	51

4.2.3	GraphSage Robustness Simulation . . . . .	55
4.3	Result Comparison . . . . .	56
<b>5</b>	<b>Discussion</b>	<b>60</b>
5.1	Informativeness of Graphs . . . . .	60
5.2	Appropriateness of Semi-Synthetic Graphs for Machine Learning . . . . .	62
5.3	GML vs. Standard ML . . . . .	63
<b>6</b>	<b>Conclusion and Outlook</b>	<b>66</b>
6.1	Conclusion . . . . .	66
6.2	Outlook . . . . .	67
<b>References</b>		<b>70</b>
<b>A</b>	<b>Simulation Results</b>	<b>78</b>
A.1	GraphSage Simulations . . . . .	78
A.2	ANN Simulations . . . . .	80
<b>B</b>	<b>Auxiliary Node2Vec Results</b>	<b>81</b>
B.1	Bank . . . . .	81
B.2	Airline . . . . .	81
<b>C</b>	<b>Various Auxiliary Results</b>	<b>83</b>
C.1	ML Bank . . . . .	83
C.2	Deterministic Graph . . . . .	83
C.3	Pairplot . . . . .	83
<b>Declaration</b>		<b>85</b>

# List of Figures

1.1	Bank Network . . . . .	3
1.2	Overview Machine Learning . . . . .	4
1.3	Overview Machine Learning Tasks . . . . .	5
2.1	Example of a Graph . . . . .	9
2.2	Network Embedding . . . . .	14
2.3	Skip-gram Architecture . . . . .	16
2.4	GNN Structure . . . . .	20
2.5	GraphSage Sampling . . . . .	23
2.6	Examples of Graph Structures that Mean and Max Aggregators Fail to Distinguish. . . . .	26
2.7	Attribute Link-Affinities . . . . .	28
2.8	Schematic Representation of the Multiplicative Attribute Graphs (MAG) Model . . . . .	28
3.1	MAG of Bank Telemarketing Dataset . . . . .	33
3.2	Biased MAG of the Bank Telemarketing Dataset . . . . .	34
3.3	Correlation Heatmap of US Airline Passenger Dataset . . . . .	36
3.4	Graph of US Airline Passenger Dataset . . . . .	40
3.5	Graph Nodes of US Airline Passenger Dataset . . . . .	41
3.6	Graph Statistics . . . . .	43
3.7	Deterministic MAG . . . . .	45
4.1	Node2Vec Embeddings . . . . .	48
4.2	GCN Loss- and Accuracy Plots . . . . .	50
4.3	Mean Aggregation Loss- and Accuracy Plots . . . . .	52
4.4	LSTM Aggregation Loss- and Accuracy Plots . . . . .	53
4.5	Sum-Pooling Aggregation Loss- and Accuracy Plots . . . . .	54
4.6	Max-Pooling Aggregation Loss- and Accuracy Plots . . . . .	54
4.7	Simulation Results Max-Pooling . . . . .	57
4.8	ANN Model Fit . . . . .	59
A.1	Simulations Results Sum-Pooling . . . . .	79
A.2	Simulation Results Mean Aggregation . . . . .	79
A.3	Simulation Results LSTM Aggregation . . . . .	80
A.4	Simulation Results ANN . . . . .	80
C.1	Max-Pooling Loss- and Accuracy Plots Deterministic MAG . . . . .	84
C.2	Pairplot Feature Data US Airline Passenger Dataset . . . . .	84

# List of Tables

3.1	Confusion Matrix Validation Bank Telemarketing Data . . . . .	33
3.2	US Airline Passenger Dataset . . . . .	37
3.3	Link-Affinity Matrices . . . . .	39
4.1	Node2Vec Classification Results . . . . .	49
4.2	Confusion Matrix Training Data GCN . . . . .	51
4.3	Confusion Matrix Validation Data GCN . . . . .	51
4.4	Test Confusion Matrix Mean Aggregation . . . . .	52
4.5	Test Confusion Matrix LSTM Aggregation . . . . .	53
4.6	Test Confusion Matrix Sum-Pooling . . . . .	54
4.7	Test Confusion Matrix Max-Pooling . . . . .	55
4.8	Simulation Results Max-Pooling . . . . .	56
4.9	Result Comparison . . . . .	58
A.1	Simulation Results Sum-Pooling . . . . .	78
A.2	Simulation Results Mean Aggregation . . . . .	78
A.3	Simulation Results LSTM Aggregation . . . . .	78
A.4	Simulation Results ANN . . . . .	80
B.1	Node2Vec Classification Results Bank Telemarketing Dataset . . . . .	81
B.2	Node2Vec Classification Results with 5-Dimensional Embeddings . . . . .	82
B.3	Node2Vec Classification Results with Feature Data . . . . .	82
C.1	Standard ML Results Bank Telemarketing Dataset . . . . .	83
C.2	Test Confusion Matrix Deterministic MAG . . . . .	84

# List of Algorithms

1	DeepWalk . . . . .	17
2	Skip-gram . . . . .	17
3	Typical GNN Algorithm for Model Training . . . . .	20
4	GraphSage Mini-batch Forward Propagation Algorithm . . . . .	24
5	Multiplicative Attribute Graph Model . . . . .	29

# List of Abbreviations

**ANN** artificial neural network

**BFS** breadth-first search

**CNN** convolutional neural network

**DFS** depth-first search

**ETF** exchange traded fund

**GAT** graph attention network

**GCN** graph convolutional network

**GIN** graph isomorphism network

**GML** graph machine learning

**GNN** graph neural network

**GPU** graphical processing unit

**GRL** graph representation learning

**KDD** Knowledge Discovery and Data Mining (International Conference)

**LSTM** long short-term memory

**MAG** multiplicative attribute graph

**ML** machine learning

**NLP** natural language processing

**OECD** Organisation for Economic Co-operation and Development

**QDA** quadratic discriminant analysis

**RNN** recurrent neural network

**SVM** support vector machine

**US** United States of America

# Chapter 1

## Introduction

This introduction chapter is meant to provide a general overview of the topic and includes the following sections:

1. General Outline
2. Motivation
3. Machine Learning Overview
4. Research Topic

First, the general outline for this master's thesis is given in the following section.

### 1.1 General Outline

The main target of this thesis is to investigate graph machine learning (GML) for the purpose of gaining customer insights. Within this general context, an emphasis is placed on the following three topics:

1. Semi-synthetic graph generation
2. Graph machine learning models
3. A comparison of the graph machine learning results with standard models.

GML is a currently very popular approach thanks to breakthrough successes of models such as AlphaFold (Senior et al. 2020). The people working at DeepMind successfully predicted protein structures with a previously unseen accuracy using the AlphaFold model. For solving the protein folding problem, the authors of AlphaFold made use of the fact, that a folded protein can be considered as a spatial graph (AlphaFold 2020). This is just an example of an area where GML can be

successfully applied. More generally, GML can be used in many different fields such as natural science, social science, and many more. An excellent overview of methods and applications for GML is given in the article by Zhou et al. (2020). This article provides a very good introduction to GML and is highly recommended to anyone unfamiliar with the topic.

What makes graphs special is their capability of capturing relationships between observations. The nodes in a graph, which correspond to the observations, may further include feature data such as labels and demographic data. GML therefore allows for the consideration of richer data. In this context, the focus of this thesis is placed on using GML for gaining customer insights. In particular, the aim is to accurately classify customers according to their type.

Generating or gaining access to graphs which contain feature data is very difficult. For that reason it is investigated to what extent, semi-synthetically generated graphs can be successfully used for machine learning (ML). To assess the success of semi-synthetic graphs, different graph based models are tested and compared to standard ML models. The specific research question is outlined in section 1.4.

This master's thesis investigates many different models and datasets. For that reason it is important to provide a general overview of the chapters present in this thesis:

**Chapter 1:** Contains the introduction for the thesis and defines the research topic.

**Chapter 2:** The required theory for understanding graphs, GML, and graph generation is presented in this chapter.

**Chapter 3:** This chapter presents the datasets and the graphs. The key findings of the datasets not considered in chapter 4, are presented in chapter 3 as well.

**Chapter 4:** Presents the ML results of the US airline passenger dataset. This dataset showed to be best suited for a fair comparison of ML models. This dataset is introduced in chapter 3 along the other datasets.

**Chapter 5:** Contains the discussion of the insights gained in chapters 3 and 4.

**Chapter 6:** Provides the conclusion and an outlook for future research.

In the following section the motivation for the topic and its relationship to business & economics is given.

## 1.2 Motivation

From a business & economics perspective graphs are particularly interesting if one wants to model the interactions between institutions. An example for this is shown in an article published by Schweitzer et al. (2009) which created the graph shown in figure 1.1. This graph depicts the relationships between international banks. Creating such a network can be a useful tool for analyzing the interdependencies between banks. In particular, it can provide important information for making the banking system more robust and resilient.

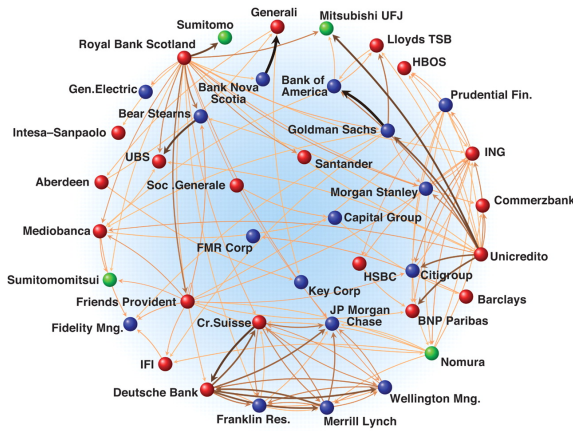


Figure 1.1: Bank Network  
(Schweitzer et al. 2009, p. 424)

Modeling social interactions is another interesting application of graphs in the field of business & economics. Social interactions can be modeled as social networks and provide valuable information for analyzing consumer behavior. This thesis will focus on gaining customer insights, which is an important and more business flavored application. Gaining customer insights has become an important topic and increasingly relies on GML. An example for this are social network companies such as Facebook and search providers like Google. Those companies mainly generate their revenue by providing customer insights and selling targeted advertising to their clients (Facebook 2021, Alphabet 2021). Both Facebook and Google have the advantage, that their businesses naturally capture network- and feature data. It is for this reason, that these companies are ideally positioned to exploit the data on their platforms using GML.

Most researchers and companies do not have access to datasets which include network information as well as feature data. In a practical setting, companies may have access to large amounts of customer data. This data however rarely contains any network information (e.g. which client is connected with which other clients).

This scenario is similar for researchers and it is especially true for social scientists which often have to collect data via anonymous surveys. This makes the collection of network information practically impossible. For that reason, companies and researchers are typically confined to working with datasets which do not contain network information. At this point it is important to mention, that there is a lot of network data available online. This network data however typically does not contain any feature data. This has the consequence, that researchers and companies have to choose between network data or feature data. For the purpose of gaining customer insights, feature data is more important. Therefore, the most practical approach is to discard network information and to focus on using features. This data access problem prevents many researchers and companies to make use of potentially superior graph based ML models. This problem motivates this master's thesis to find alternatives which at least in part remove the barrier for GML. For that reason, alternative graph generation procedures are investigated and are presented along with the research topic in section 1.4.

Before presenting the research topic, a general overview of the ML models used in this thesis is given in the following section.

## 1.3 Machine Learning Overview

This section provides a high-level overview of machine learning (ML) and specifies the type of ML task used in this thesis. To start, it is important to correctly categorize ML. There are many related big topics such as data science, big data, and artificial intelligence and it is often not clear what exactly is meant. An overview of how these different terms can be categorized is shown in figure 1.2.

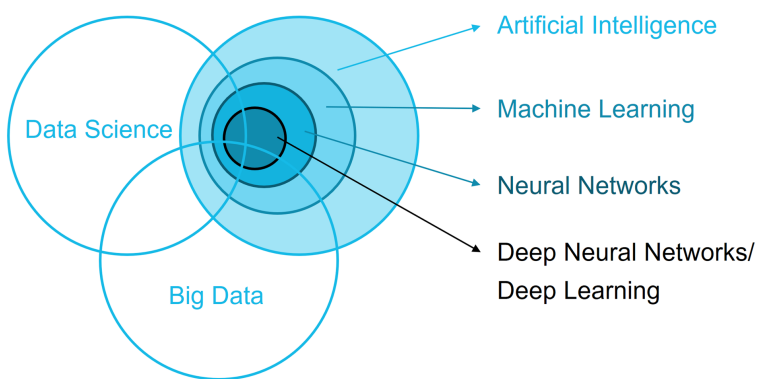


Figure 1.2: Overview Machine Learning  
(Frauenhofer Institut 2021)

Figure 1.2 depicts well, how these different terms are related with each other. ML in

particular is mostly ascribed to the domain of artificial intelligence. It however also has a shared domain with data science and big data. It is thus at the intersection of these three interrelated fields. ML models such as neural networks and deep neural networks are specific models within ML and are often referred to separately due to their popularity. In this thesis, differentiating between ML and neural networks is not necessary, as the considered ML models are used for the same task. ML can be applied for various tasks and is again best presented visually as shown in figure 1.3.

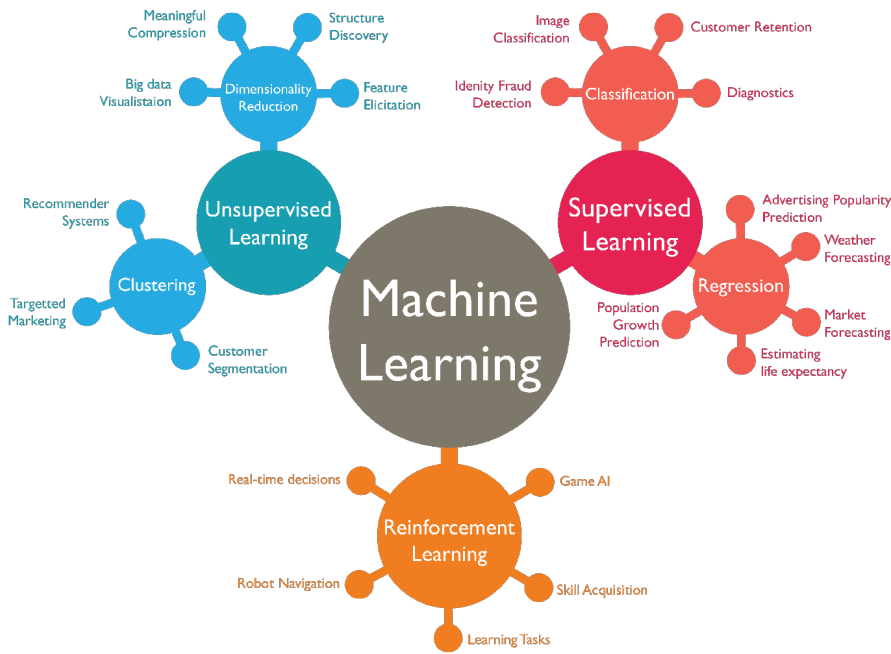


Figure 1.3: Overview Machine Learning Tasks  
(Artisan's Asylum 2020)

It is shown in figure 1.3, that the main tasks for ML involve classification, regression, reinforcement learning, clustering, and dimensionality reduction. This thesis focuses on classification tasks. This task is chosen given the available data and because it allows for a nice comparison of different ML models. Well known standard ML models used for classification tasks include logistic regression (Cramer 2002), naive bayes (Zhang 2004), support vector machines (SVMs) (Platt et al. 1999), random forest classifiers (Breiman 2001), AdaBoost (Freund & Schapire 1997), quadratic discriminant analysis (QDA) (Tharwat 2016) and artificial neural networks (ANNs) (McCulloch & Pitts 1943, Werbos 1974). This is an incomplete list of popular ML models that can be used for classification tasks. Well-known applications of classification tasks include predicting whether a customer is satisfied, whether to grant a mortgage to a client, and many more. The aforementioned ML models have in common, that they can only consider feature data. It is in general not possible to directly make use of network information for these models.

GML models are special because they can consider both feature data as well as network information. Using the overview shown in figure 1.2, GML is probably best categorized as a special form of neural network. It is however not a deep neural network, as network depth does not necessarily improve the model and can be even counter-productive. Within GML there are two main approaches. The first approach focuses on learning vector representations of graphs which are then used for downstream ML. The downstream ML models involve the standard models presented previously. These Graph representation learning (GRL) approaches include models such as DeepWalk (Perozzi et al. 2014) and Node2Vec (Grover & Leskovec 2016) among others. The second approach involves the application of graph neural networks (GNNs) for which there exist many different models. Popular and established models include graph convolutional networks (GCNs) (Kipf & Welling 2016) and GraphSage (Hamilton et al. 2017). The detailed theoretical background for the considered GML models is provided in chapter 2.

## 1.4 Research Topic

The difficult access to graphs which also contain features motivates the search for alternatives. A review of the literature revealed, that a form of synthetic graph generation could provide a solution to the data access problem. Classic graph generation models include the famous Erdös-Rényi graphs (1959), the small-world model by Watts & Strogatz (1998), the well-known model by Barabási & Albert (1999), and more recently Kronecker graphs by Leskovec et al. (2010). These models are all very instructive regarding the graph generation process and for understanding graph properties. These networks however all have the short-coming, that they do not allow for the assignment of feature data to the nodes/observations in the network. It became clear, that one has to find or develop a model which makes use of existing feature data for the graph generation process. Kim & Leskovec (2012) developed the multiplicative attribute graph (MAG) model. This model makes use of randomly generated feature data which is referred to as attribute data by the authors. The model is shown to be capable of generating random graphs which can adhere to observed real world network properties. An analysis of the MAG model revealed, that it could also be a useful model for creating semi-synthetic graphs using existing feature data. For that reason, the MAG model is chosen for generating semi-synthetic graphs. This model is introduced in detail in section 2.3.

More recently, researchers have focused their attention on deep generative graph models. These models create graphs with features using real graphs as a training input. Examples for such models are graph recurrent neural networks (You et al.

2018) and deep generative graph models (Li et al. 2018). These are very fascinating models which can be used to recreate or scale graph data. For the purpose of this thesis, these models are not useful as it requires an existing graph with features to be available. Such a graph was unfortunately not available for writing this master’s thesis. Nevertheless, this is an interesting current topic for graph generation which was considered.

The MAG model is interesting as it could allow for the creation of semi-synthetic graphs using feature data. Semi-synthetic refers to the fact, that the graph is generated using real feature data. A fully synthetic graph would be generated using completely artificial data. Many companies and researchers have access to large feature datasets. These datasets include customer databases or collected survey data. For that reason it would be of great benefit, if the MAG model could generate useful semi-synthetic graphs. The usefulness of a graph is determined to the extent, that the graph can be used for ML and yield a high accuracy for a given classification task. It is not expected, that the semi-synthetic graphs can fully substitute real graphs. Real world networks often capture relationships, which are difficult to formalize and thus recreate using approaches such as the MAG model. Nevertheless, the semi-synthetic graphs could be capable of generating useful network information. If this holds true, the semi-synthetic graph contains richer data which can then be exploited using GML. To assess the viability of this approach, the results using semi-synthetic graphs should be able to outperform or at least compete with the results using standard ML models. Therefore to assess these hypotheses, the results using GML are compared to the results using standard ML models. To close this section and chapter, the research question as well as the hypotheses of this thesis are presented formally as follows.

### **Research Question**

To what extent are semi-synthetic graphs based on real feature data useful for a classification task using graph machine learning?

### **Hypotheses**

**H1:** Graph machine learning models using semi-synthetic graphs provide superior results compared to the results of standard machine learning models for a given classification task.

**H2:** Graph machine learning using semi-synthetic graphs is a competitive strategy compared to the results of standard machine learning models for a given classification task.

# Chapter 2

## Theory

This chapter covers the required theoretical background and consists of the following main parts:

1. Graph Theory
2. Machine Learning on Graphs
3. Graph Generation

### 2.1 Graph Theory

This section provides a brief introduction to graph theory with a focus on the relevant aspects for this master's thesis. The theory presented in this section is primarily taken from the book "Networks: An Introduction" by Mark Newman (2010).

Graph theory is an old field of mathematics and can be traced back to Leonhard Euler and the famous "Königsberg Bridge Problem" (Euler 1736). The study of graphs has had a recent revival thanks to its useful applications in areas such as the Google algorithm PageRank (Page et al. 1999) and GML. Graphs are special data structures for which an example is shown in Figure 2.1. The terms graph and network are often used interchangeably and have the identical meaning for the purpose of this master's thesis. Typically, the term graph is used more commonly for the mathematical analysis of graphs and the term network is more commonly used in data science.

The graph shown in Figure 2.1 corresponds to an undirected graph in which the connections between the vertices are mutual. In a directed graph for instance, vertex A could be connected to vertex B, however vertex B need not be connected to vertex A. For the purpose of this thesis, only undirected graphs are considered. Vertices are often referred to as nodes and the terms are used interchangeably. Edges refer

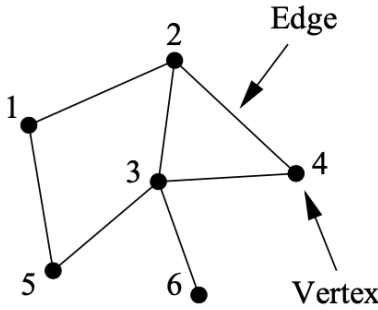


Figure 2.1: Example of a Graph  
(Newman 2010, p. 111)

to the connections between the vertices. The term links is also often used to refer to edges and the terms are used interchangeably as well. Graphs may have additional elements such as multi-edges or self-edges. Self-edges refer to nodes which have a looped link to themselves. This can be considered as a form of feedback loop of a node on to itself. Lastly, multi-edges refer to direct node connections with multiple paths. For notation purposes, graphs are typically defined as follows:

$$G(V, E) \quad (2.1)$$

$G$  denotes the graph,  $V$  refers to the set of vertices present in the graph, and  $E$  refers to edges present between the vertices.

This concludes the basic setup of graphs. The following paragraphs give an introduction to the adjacency matrix, the node degrees, and the centrality measures which are used in this thesis.

### Adjacency Matrix

The adjacency matrix  $A$  is defined as a  $n \times n$  matrix, where  $n$  refers to the number of vertices present in the graph. Each vertex is therefore recorded by a column and a row in the adjacency matrix. The elements in the adjacency matrix are further typically defined as follows:

$$A_{ij} = \begin{cases} 1, & \text{if vertex } i \text{ and } j \text{ are connected by an edge} \\ 0, & \text{otherwise} \end{cases} \quad (2.2)$$

For illustration, the adjacency matrix of the graph depicted in Figure 2.1 is shown as follows:

$$A = \begin{pmatrix} 0 & 1 & 0 & 0 & 1 & 0 \\ 1 & 0 & 1 & 1 & 0 & 0 \\ 0 & 1 & 0 & 1 & 1 & 1 \\ 0 & 1 & 1 & 0 & 0 & 0 \\ 1 & 0 & 1 & 0 & 0 & 0 \\ 0 & 0 & 1 & 0 & 0 & 0 \end{pmatrix}$$

As one can see in the adjacency matrix, if vertex  $i$  and  $j$  are connected, this is recorded with 1 and 0 otherwise. Note, that all of the elements on the  $\text{diag}(A)$  are equal to 0. This is because there are no self-edges present in figure 2.1. Nodes with self-loops would have a 1 recorded on the corresponding diagonal element of the adjacency matrix. In addition, multi-edges can be recorded with the number of edges present between two vertices. For example, vertices which are connected by two edges would be recorded with a 2 in the adjacency matrix. The graph shown in figure 2.1 is an undirected network. For that reason, the adjacency matrix is symmetric. The adjacency matrix can further be used for representing different types of graphs such as weighted networks. These aspects are however not relevant for this thesis. For additional information regarding the adjacency matrix, again the book by Mark Newman (2010) is highly recommended.

### Degree Measures

An important measure for graphs are the vertex degrees denoted by  $k$ . Degrees refer to the number of edges connected to a vertex. The degrees of vertex  $i$  can be formulated as (Newman 2010, p. 133):

$$k_i = \sum_{j=1}^n A_{ij} \tag{2.3}$$

For an undirected graph, edges have two ends. This is due to the fact, that vertices connected by an edge are mutually connected. To calculate the sum of the degrees of all vertices, one can therefore write for an undirected graph with  $m$  edges and  $n$  vertices (Newman 2010, p. 133):

$$2m = \sum_{i=1}^n k_i \tag{2.4}$$

As a statistical measure, the mean degree  $c$  of a vertex is defined as follows (Newman 2010, p. 134):

$$c = \frac{1}{n} \sum_{i=1}^n k_i = \frac{2m}{n} \tag{2.5}$$

To calculate the density of a graph, it should first be noted, that the maximum number of edges is given by (Newman 2010, p. 134):

$$\binom{n}{2} = \frac{1}{2}n(n - 1) \quad (2.6)$$

The density  $\rho$  can thus be written as (Newman 2010, p. 134):

$$\rho = \frac{m}{\binom{n}{2}} = \frac{2m}{n(n - 1)} = \frac{c}{n - 1} \quad (2.7)$$

Note, that the density  $\rho$  lies strictly between  $0 \leq \rho \leq 1$ . In addition, for sufficiently large graphs, one can approximate  $\rho = \frac{c}{n}$ .

### Eigenvector Centrality

The degrees of a vertex shown in the previous section correspond to the simplest form of a centrality measure. The issue with this measure is, that every neighbor of vertex  $i$  is valued the same. This is a problem, as not all neighbors are of equal importance due to:

1. The number of the neighbor's neighbors
2. The importance of the neighbor
3. Both

There are many different alternative centrality measures which can consider the factors listed above such as eigenvector centrality, Katz centrality, and PageRank (Landau 1895, Katz 1953, Page et al. 1999). For analyzing undirected graphs, eigenvector centrality is sufficient and is presented in more detail.

Eigenvector centrality gives all vertices a centrality score which is proportional to the sum of the scores of the vertices' neighbors  $j$ . This is a procedure in which typically the initial centrality  $x_i$  of vertex  $i$  is guessed to be  $1 \forall i$ . This can be used to calculate the centralities of the neighbors of  $i$  which is denoted by  $x'_i$ . One can thus write (Newman 2010, p. 169):

$$x'_i = \sum_j A_{ij}x_j \quad (2.8)$$

In matrix notation:

$$x' = Ax \quad (2.9)$$

This process is repeated  $t$  times as follows to generate better estimates (Newman 2010, p. 170):

$$x(t) = A^t x(0), \quad (2.10)$$

where  $x(0)$  denotes the linear combination of (Newman 2010, p. 170):

$$x(0) = \sum_i c_i v_i \quad (2.11)$$

The variable  $v_i$  denotes the eigenvectors of the adjacency matrix  $A$  and  $c_i$  corresponds to an appropriately chosen constant. Therefore one can write (Newman 2010, p. 170):

$$x(t) = A^t \sum_i c_i v_i = \sum_i c_i k_i^t v_i = k_1^t \sum_i c_i \left[ \frac{k_i}{k_1} \right]^t v_i \quad (2.12)$$

In equation 2.12,  $k_i$  correspond to the eigenvalues of the adjacency matrix  $A$ .  $k_1$  corresponds to the largest eigenvalue of  $A$ . As  $\frac{k_i}{k_1} < 1, \forall i \neq 1$ , the term is decaying as  $t \rightarrow \infty$ . The centralities  $x$  can therefore be written in terms of fulfilling following condition (Newman 2010, p. 170):

$$Ax = k_1 x \quad (2.13)$$

Thus, the eigenvector centrality is defined as (Newman 2010, p. 170):

$$x_i = k_1^{-1} \sum_j A_{ij} x_j \quad (2.14)$$

### Closeness Centrality

The closeness centrality  $C_i$  of vertex  $i$  is defined as the average distance to the other vertices  $j$  in the graph. This centrality measure is defined as follows (Newman 2010, p. 182):

$$C_i = \frac{1}{l_i} = \frac{n}{\sum_j d_{ij}} \quad (2.15)$$

For this measure, central vertices exhibit high closeness centrality and are therefore more closely connected to the other vertices compared to vertices with low closeness centrality. The variable  $l_i$  denotes the average geodesic distance  $d_{ij}$  of vertex  $i$ . The range of the closeness centrality lies within the range  $0 \leq C_i \leq 1$ .

### Betweenness Centrality

This centrality measures to which extent a vertex  $i$  lies on a geodesic path between two other vertices. For instance, a bottleneck vertex would exhibit a large betweenness centrality if many nodes must pass through it to reach their destination. More

formally, betweenness centrality  $x_i$  is defined as (Newman 2010, p. 187):

$$x_i = \sum_{st} \frac{\eta_{st}^i}{g_{st}} \quad (2.16)$$

In equation 2.16,  $\eta_{st}^i$  refers to the number of geodesic paths from  $s$  to  $t$  which pass through vertex  $i$ . Further,  $g_{st}$  is defined as the number of geodesic paths between vertex  $s$  and  $t$ .

In order to allow for a better comparison of betweenness centralities, it is often standardized by the number of connected vertex pairs  $s$  and  $t$  denoted by  $\eta^2$ . The betweenness centrality in its standardized form can thus be written as (Newman 2010, p.190):

$$x_i = \frac{1}{\eta^2} \sum_{st} \frac{\eta_{st}^i}{g_{st}} \quad (2.17)$$

With this measure, the betweenness centrality is within the range  $0 \leq x_i \leq 1$ .

## 2.2 Machine Learning on Graphs

Graphs are special because the nodes/datapoints in a graph are linked with each other. A practical example for this are social networks. In a social network, the profiles of "Peter" and "Paul" might be connected because "Peter" and "Paul" are friends. In addition, "Paul" and "Peter" can only ever reach each other, if they are directly or perhaps indirectly connected via a mutual friend. This aspect is unique to network data and provides interesting additional information as well as added complexity. This property does not allow for comparing the nodes in a graph using common distance measures such as Euclidean distances. The edges connecting the nodes only indicate that two nodes are connected. It however does not indicate whether two connected nodes are more- or less similar compared to two other connected nodes. In addition, how similar are indirectly connected nodes? Further, how similar or dissimilar are these nodes compared to other indirectly connected nodes? This rapidly becomes a very complex question. The challenge is thus to develop a model which can accurately measure the similarities of the nodes present in a graph. GML provides solutions to this problem and can be grouped into the following two main categories:

1. Graph representation learning
2. Graph neural networks

Graph representation learning refers to models which generate node embeddings of a given graph. Specifically, this approach creates vector representations of the nodes in a graph given a defined similarity measure. For these node vector representations, distance measures such as Euclidean distances can be measured. The generated node embeddings can thus be used for downstream ML using standard models. A graph neural network can also generate node embeddings as well as directly using graphs for a given classification task among others. The capability of directly applying graphs for ML makes GNNs especially promising.

In the following two subsections the theory for GRL and GNNs is introduced. The theory presented in these subsections is in part based on the CS224W lecture<sup>1</sup> at Stanford University given by Prof. Dr. Jure Leskovec (2021).

### 2.2.1 Graph Representation Learning

The aim of graph representation learning (GRL) is to generate node embeddings in the form of  $d$ -dimensional vector representations. The resulting node embeddings can then be used for standard ML applications. A graphical representation of this task is shown in figure 2.2.

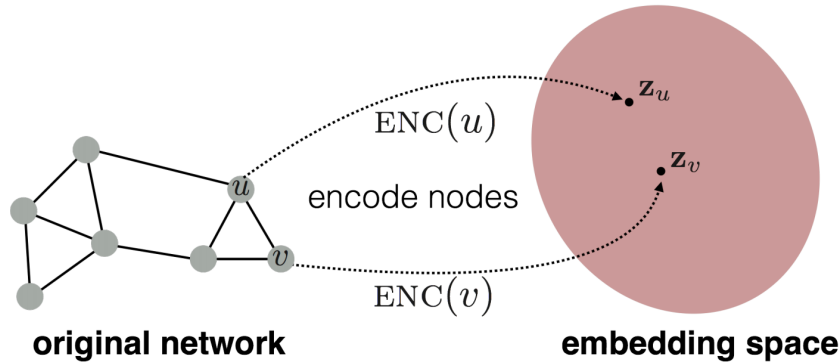


Figure 2.2: Network Embedding  
(Leskovec 2021)

To generate node embeddings of a graph, one has to define an encoder which transforms nodes in a graph into their embedding space as shown in figure 2.2. The nodes must be embedded in such a manner that similar nodes in the graph are also embedded closely together in the embedding space. A common measure for similarity is to find vector embeddings  $z$  of nodes  $u$  and  $v$  such that (Leskovec 2021):

$$z_u^T z_v \approx \text{similarity}(u, v) \quad (2.18)$$

<sup>1</sup>CS224W website: <http://web.stanford.edu/class/cs224w/>

The dot product of the two node embedding vectors shown in equation 2.18 should thus approximately equal the similarity of the corresponding nodes in the graph. There are different approaches for defining node similarity. Graph factorization was introduced as an early solution (Ahmed et al. 2013). More recent and successful approaches include methods which make use of random walks. In the context of random walks, similarity is defined as (Leskovec 2021):

$$z_u^T z_v \approx \text{Probability that node } u \text{ and } v \text{ co-occur on a random walk over the graph} \quad (2.19)$$

The models DeepWalk (Perozzi et al. 2014) and its generalization Node2Vec (Grover & Leskovec 2016) successfully apply the similarity measure shown in equation 2.19. Another noteworthy model called LINE (Tang et al. 2015) also makes use of random walk co-occurrences as its similarity measure. In order to remain focused, only DeepWalk and Node2Vec are considered for this thesis. These two models are well suited for the given task and are among the most popular GRL models.

DeepWalk and Node2Vec make use of methods which have its origin in natural language processing (NLP). More specifically, they makes use of the Skip-gram model introduced by Mikolov et al. (2013a,b). The Skip-gram model is a core component of DeepWalk and Node2Vec, which is why it is explained in detail before proceeding to the GRL models.

In NLP words are one-hot encoded as inputs for the Skip-gram model which learns vector representations of the input words. The aim of the Skip-gram model is then to predict the context of the input word by predicting the neighboring words in a sentence. A basic overview of the Skip-gram model is provided in figure 2.3.

The basic layout shown in figure 2.3 depicts the high-level procedure of the Skip-gram model. To make this model more specific, the input corresponds to the one-hot encoded vector at row  $t$  of the input matrix  $W$  with dimensions  $T \times T$ , where every row corresponds to a one-hot encoded word.  $W(t)$  is linearly passed to the projection, which involves calculating the dot product of  $W(t)$  with the weight matrix  $\Phi$  which has dimensions  $T \times D$ .  $D$  refers to the number of dimensions which are to be included in the projection vector  $h$  and is a hyper parameter. The projection vector  $h$  is then linearly passed again with another weight matrix  $\Psi$  which has dimensions  $D \times T$ . This creates the output vector  $u$  which is then used to predict the correct context word  $c$  from the vocabulary of  $C$  number of context words. To do so, the training target is set to maximize the average log probability of the correct context word for every input word  $w_t$ .

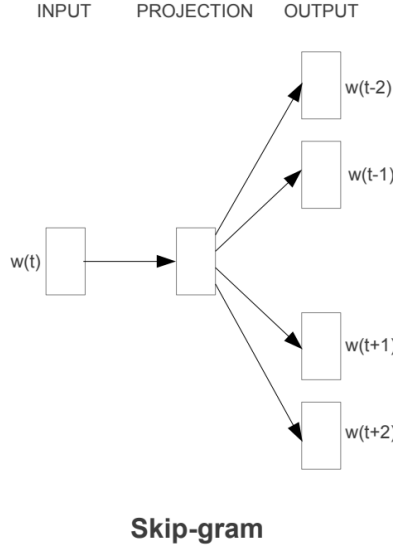


Figure 2.3: Skip-gram Architecture  
(Mikolov et al. 2013a, p. 5)

The average log probability is more formally defined by (Mikolov et al. 2013b, p. 2):

$$\frac{1}{T} \sum_{t=1}^T \sum_{-c \leq j \leq c, j \neq 0} \log p(w_{t+j} | w_t) \quad (2.20)$$

To calculate the probability of the context word given the input word  $w_t$ , the softmax function (Bridle 1990a,b) is applied to the output layer  $u$  in the manner shown by Mikolov et al. (2013b, p. 3). This calculates a normalized probability for every context word given  $w_t$ . To formalize this in terms of a loss function, the training target shown in equation 2.20 can be rewritten as follows for every input word  $w_t$ :

$$\begin{aligned} \mathcal{L} &= -\log p(w_{t-c}, \dots, w_{t-1}, w_{t+1}, \dots, w_{t+c} | w_t) \\ &= -\log \prod_{c=1}^C \frac{\exp(u_{c,j_c^*})}{\sum_{j'=1}^T \exp(u_{j'})} \\ &= -\sum_{c=1}^C u_{j_c^*} + C \cdot \log \sum_{j'=1}^T \exp(u_{j'}) \end{aligned} \quad (2.21)$$

The notation was slightly adjusted, where  $u_{j_c^*}$  refers to the index of the output vector  $u$  which corresponds to the actual context word  $c$  given the input word  $w_t$ . In turn,  $\sum_{j'=1}^T \exp(u_{j'})$  is a summation over all exponentiated output representations  $u_{j'}$  of all  $T$  number of words given the input word  $w_t$ . The calculated loss is then

used to update the trainable model parameters  $\Phi$  and  $\Psi$  using gradient descent via a backward propagation function (Werbos 1974) analogues to what is used for standard neural networks. The desired output of the Skip-gram model is the weight matrix  $\Phi$  which once the model is sufficiently trained, corresponds to the vector representation or embeddings of the input words.

The same principle shown in the Skip-gram model can be applied to graphs in a modified version. First, nodes in a graph can be one-hot encoded the same way as words. This means, that nodes can be used as input data in a similar fashion as words. Based on this idea, DeepWalk by Perozzi et al. (2014) achieved a big breakthrough for GRL. The DeepWalk algorithm builds on top of the Skip-gram model and uses fixed-length random walks for learning the node embeddings. To provide a better overview of the DeepWalk algorithm, the pseudo-code is presented in algorithms 1 & 2 (Perozzi et al. 2014, p. 704).

---

**Algorithm 1:** DeepWalk( $G, w, d, \gamma, t$ )

---

```

Input: graph  $G(V, E)$ 
window size  $w$ 
embedding size  $d$ 
walks per vertex  $\gamma$ 
walk length  $t$ 
Output: matrix of vertex representations  $\Phi \in \mathbb{R}^{|V| \times d}$ 
1 Initialization: Sample  $\Phi$  from  $\mathcal{U}^{|V| \times d}$ 
2 Build a binary Tree  $T$  from  $V$ 
3 for  $i = 0$  to  $\gamma$  do
4    $\mathcal{O} = \text{Shuffle}(V)$ 
5   foreach  $v_i \in \mathcal{O}$  do
6      $\mathcal{W}_{vi} = \text{RandomWalk}(G, v_i, t)$ 
7     SkipGram( $\Phi, \mathcal{W}_{vi}, w$ )
  end
end

```

---



---

**Algorithm 2:** SkipGram( $\Phi, \mathcal{W}_{vi}, w$ )

---

```

1 foreach  $v_j \in \mathcal{W}_{vi}$  do
2   foreach  $u_k \in \mathcal{W}_{vi}[j - w : j + w]$  do
3      $J(\Phi) = -\log \Pr(u_k | \Phi(v_j))$ 
4      $\Phi = \Phi - \alpha * \frac{\partial J}{\partial \Phi}$ 
  end
end

```

---

The DeepWalk algorithm shows, that for every node  $v \in G$  a fixed length random walk is created. Every node on the random walk is used as a one-hot encoded input for the Skip-gram model. The context nodes of the input node correspond to the input nodes' neighbors on the random walk within the window size  $w$ . This procedure is repeated for  $\gamma$  number of random walks which in turn concludes one training epoch. The rows of  $\Phi$  then correspond to the node embeddings where  $\Phi_u = z_u^T$ . Lastly, the dot product of any two node embedding vectors,  $z_u^T z_v$ , approximately equals the probability, that the two nodes co-occur on a random walk as outlined in

equation 2.19. Please note, that the DeepWalk algorithm often uses more efficient approximation methods to calculate the loss function shown in equation 2.21. These approximation methods include hierarchical softmax which makes use of a binary tree or negative sampling. Both approximation methods are outlined in the paper by Mikolov et al. (2013b).

This is in principle the model which will be used to find the node embeddings of a graph. For the application, the Node2Vec algorithm by Grover & Leskovec (2016) will be employed, which is a generalization of the DeepWalk algorithm. Node2Vec allows for the deployment of biased random walks. In particular, it allows to set probabilities as to whether the random walk is biased towards breadth-first search (BFS) or depth-first search (DFS). Depending on the network structure, setting an appropriate bias can greatly improve the quality of the embeddings. If no bias towards BFS or DFS is set, an unbiased random walk is employed which is when the output of the Node2Vec algorithm corresponds to the output of the DeepWalk algorithm. More precisely, this occurs when the search bias is set to  $\alpha = 1$  with  $p = q = 1$  as outlined in the Node2Vec paper (Grover & Leskovec 2016, p. 860). The results revealed, that an unbiased random walk embedded the nodes very well. For that reason, the Node2Vec algorithm is not explained in further detail as the relevant parts are covered by the simpler and reader friendlier DeepWalk algorithm. If interested, the pseudo-code for the Node2Vec algorithm is provided in the article by Grover & Leskovec (2016, p. 859).

The resulting node embeddings can then be used for downstream ML tasks using standard models. An additional benefit of GRL is that the nodes can be encoded into an arbitrary number of dimensions. In this sense, GRL can be used as a powerful dimensionality reduction strategy. The node embeddings correspond to the feature data used for the downstream ML tasks. The features were thus learned automatically using the DeepWalk or Node2Vec algorithm. This approach directly takes care of the otherwise at times tedious feature selection process. With this approach, only the number of features need to be defined for feature selection. This is a big advantage and can save a lot of time when working with graphs.

## 2.2.2 Graph Neural Networks

This section provides an overview of the theory for graph neural networks (GNNs). Within the family of GNNs, there are a myriad of different models available and every few months new models are published. GNNs are currently very popular and benefit from a large research output. This thesis will focus on two popular and

established GNN approaches which are:

1. Graph Convolutional Networks
2. GraphSage

Before presenting the two above mentioned methods, a general overview of the GNN framework is given. First, the required setup is defined (Leskovec 2021):

- $G(V, E)$  is a graph with a set of vertices and edge connections
- $V$  is a set of vertices
- $A$  is the adjacency matrix of graph  $G$
- $X \in \mathbb{R}^{|V| \times F}$  is a matrix containing the node features
- $v$  is a node  $\in V$  and  $\mathcal{N}(v)$  is the set of neighbors of node  $v$

If there are no node features present,  $X$  can be defined as a one-hot encoded vector. A naive approach for building a GNN would be to append the columns of the adjacency matrix to the feature matrix. This combined matrix would then be used as the input for a standard ANN. The problem with this approach is, that the input is not order invariant and that the trained model cannot be applied to graphs of different sizes (Leskovec 2021).

Modern GNNs have overcome this problem by drawing inspiration from convolutional neural networks (CNNs) and its famous filtering mechanism as outlined by Krizhevsky et al. (2012). CNNs typically work with grid structured input data such as pixels of images. The convolutional filter then samples the input grid using a filter with a specified size (e.g.  $3 \times 3$  grid filter). Similarly, GNNs sample a graph using the node neighbors  $\mathcal{N}(v)$  of node  $v$  as a filter. The filter can then be fine tuned in the sense of how many  $k$ -hops of neighbors to consider (e.g. 1-hop: immediate neighbors of  $v$ , 2-hop: include neighbors of  $v$ 's neighbors etc.). In terms of implementation, the number of  $k$ -hops is set by the number of graph convolutional layers included in the GNN model. An illustration of this mechanism is shown in figure 2.4.

The GNN structure outlined in figure 2.4 shows an example of a 2-hop or 2 layer GNN. The 1-hop convolutional layer considers the neighboring nodes of the target node A. The 2-hop layer considers the neighbors of node A's neighbors. Note, that the target node A is included as an input node in the 2-hop layer. This is reasonable as node A itself is also a neighboring node to its neighbors. Taking the example shown in figure 2.4, the challenge for the GNN is to find node embeddings based

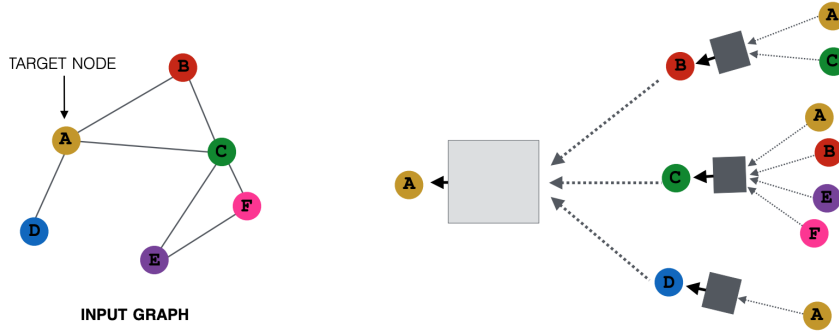


Figure 2.4: GNN Structure  
(Leskovec 2021)

on local network neighborhoods (Leskovec 2021). The node embeddings at layer 0 correspond to the features of the input nodes where  $X = H^{(0)}$ . A typical procedure for a GNN model is outlined in the pseudo-code shown in algorithm 3 (Hamilton et al. 2017, Leskovec 2021, You et al. 2020).

---

**Algorithm 3:** Typical GNN Algorithm for Model Training

---

**Input:** Graph  $G(V, E)$ ;  
 input features  $\{x_v, \forall v \in V\}$ ;  
 node labels  $\{y_v, \forall v \in V\}$ ;  
 depth/layers  $K$   
 Trainable and layer specific parameters  $\Theta^k$  where  $W^k \in \Theta^k, \forall k \in \{1, \dots, K\}$ ;  
 non-linearity  $\sigma$ ;  
 differentiable aggregator functions  $AGGREGATE_k, \forall k \in \{1, \dots, K\}$ ;  
 neighborhood function  $\mathcal{N}_k : v \rightarrow 2^V, \forall k \in \{1, \dots, K\}$ ;  
 loss function  $\mathcal{L}$  such as cross entropy  $CE$ ;  
 learning rate  $\alpha$

**Output:** Vector representations  $z_v, \forall v \in V$

- 1 Initialize parameters  $\Theta$  from  $\mathcal{U}$ ;
- 2  $h_v^0 = x_v, \forall v \in V$
- 3 **for** Number of epochs **do**
- 4     **for**  $k = 1 \dots K$  **do**
- 5         **forall**  $v \in V$  **do**
- 6              $h_{\mathcal{N}(v)}^k \leftarrow AGGREGATE_k(h_u^{k-1}, \forall u \in \mathcal{N}_k(v))$ ;
- 7              $h_v^k \leftarrow \sigma(W^k \cdot CONCAT(h_v^{k-1}, h_{\mathcal{N}(v)}^k))$ ;
- 8         **end**
- 9          $h_v^k \leftarrow h_v^k / \|h_v^k\|_2$
- 10     **end**
- 11      $z_v = h_v^K, \forall v \in V$ ;
- 12      $\mathcal{L}(\Theta) = \sum_{v=1}^{|V|} CE(y_v, z_v)$ ;
- 13      $\Theta = \Theta - \alpha \cdot \frac{\partial \mathcal{L}}{\partial \Theta}$
- 14 **end**

---

Algorithm 3 is not meant to be considered as a complete overview and should be rather regarded as an example of a typical GNN structure. In addition, one should split the data into training- and validation sets to ensure a good model fit. GNNs are flexible in that a myriad of modifications can be added to the GNN layers similar to the possibilities of CNNs and ANNs. The defining features of different GNN models usually involve the selection of different message passing methods and aggregation

strategies. An excellent overview regarding the design space for GNNs is provided in the articles by You et al. (2020) and Zhou et al. (2020) as a reference. Of course, there are exceptions and alternative procedures exist. The GNN models evaluated in this thesis and most successful GNNs however tend to follow a variation of the structure shown in algorithm 3.

In terms of interpretation, the output of the first GNN layer in figure 2.4 (gray boxes) corresponds to the hidden layer representations of the direct neighbors of the target node A. The output of the final GNN layer corresponds to the node embedding  $z_A$  of the target node A. This should appear familiar when comparing this approach to the GRL models introduced in the previous section. GNNs can indeed be used for unsupervised learning tasks such as learning node embeddings. Good examples for generating node embeddings are shown in the articles regarding GCNs by Kipf & Welling (2016) and GraphSage by Hamilton et al. (2017). As shown in algorithm 3, GNNs can directly be applied for ML tasks such as customer classification. This is where GNNs are especially powerful and differ to the GRL algorithms outlined in the previous section. GNNs are flexible tools and can be used in various settings such as GRL, clustering, classification and link prediction tasks among others (Zhou et al. 2020).

Having introduced the general functionality of GNNs, the models GCN and GraphSage are introduced in detail in the following two sections.

### 2.2.2.1 Graph Convolutional Networks

The graph convolutional network (GCN) was introduced by Kipf & Welling (2016) and makes use of simplified spectral graph convolutions. The author Thomas Kipf (2016) provides excellent explanations on his website<sup>2</sup> which is used as inspiration for presenting the theory. As outlined, GNNs typically differ with regards to the type of message passing and aggregation strategy applied. GCNs make use of the following forward propagation function (Kipf & Welling 2016, p. 2):

$$H^{(l+1)} = \sigma \left( \tilde{D}^{-\frac{1}{2}} \tilde{A} \tilde{D}^{-\frac{1}{2}} H^{(l)} W^{(l)} \right) \quad (2.22)$$

The variables in equation 2.22 are defined as follows:

- $H^l \in \mathbb{R}^{N \times D}$  refers to the embedding matrix at layer  $l$  where  $N$  refers to the number of nodes  $|V|$  and  $D$  refers to the number of embedding dimensions. The input embedding matrix is set equal to the feature matrix,  $H^{(0)} = X$ .

---

<sup>2</sup>Website Thomas Kipf: <https://tkipf.github.io/graph-convolutional-networks/>

- $W^l$  refers to the trainable and layer specific weight matrix for the linear message passing employed in the GCN model.
- $\tilde{A} = A + I_N$ , where  $A$  is the adjacency matrix of the input graph  $G$ . The identity matrix is added so that self-loops are considered. This is necessary as the target node of every layer is considered in the aggregation process as previously outlined.
- $\tilde{D}_{ii} = \sum_j \tilde{A}_{ij}$  is a diagonal matrix containing the degree distributions of the modified adjacency matrix  $\tilde{A}$ .
- $\sigma(\cdot)$  refers to an activation function such as ReLU (Nair & Hinton 2010) or softmax.

To provide a better overview, the compact notation shown in equation 2.22 is expanded in the following equation for one GCN layer (Dubois 2019):

$$h_{ij}^{(l)} = \sigma \left( \sum_{(i,j) \in \mathcal{N}(v)} \frac{\tilde{a}_{ik} h_{kj}^{(l-1)}}{\sqrt{\tilde{d}_{k,k} \tilde{d}_{i,i}}} W^{(l)} \right) \quad (2.23)$$

In Equation 2.23  $h_{ij}^{(l)}$  refers to the hidden layer representation of node  $i$  at layer  $l$  considering the set of neighbors  $j$ .  $h_{kj}^{(l-1)}$  corresponds to the hidden layer representation of node  $k$  at layer  $l - 1$  which is part of the set of neighbors  $j$ . In terms of filtering strategy,  $(i, j) \in \mathcal{N}(v)$ . This means that both set of nodes  $i$  and  $j$  are neighbors of the target node  $v$  at layers  $l$  and  $(l - 1)$  respectively. Linear message passing is then performed for every neighbor in  $j$  at layer  $l - 1$ . The node in the graph  $G$  at position  $\tilde{a}_{ik}$  of the modified adjacency matrix selects the nodes for which a connection between  $h_{ij}^{(l)}$  and  $h_{kj}^{(l-1)}$  exists. The embeddings  $h_{kj}^{(l-1)}$  of the selected nodes are normalized by the symmetric degree distributions of the previous hidden layer node  $\tilde{d}_{k,k}$  and the new hidden layer node  $\tilde{d}_{i,i}$ . Afterwards the normalized embeddings are message passed by multiplying it with the shared weight matrix  $W^{(l)}$ . Lastly, the sum of the received messages is taken in terms of aggregation strategy and the resulting aggregate is passed through the activation function to yield  $h_{ij}^{(l)}$ . Note, that the aggregation strategy involves taking a weighted sum thanks to the symmetric normalization.

The detailed explanations given above show the procedure for one layer of a GCN. Returning now to compact notation, this procedure can be expanded for two or more GCN layers. First, the notation is further simplified by defining  $\hat{A} = \tilde{D}^{-\frac{1}{2}} \tilde{A} \tilde{D}^{-\frac{1}{2}}$ . An example of a two layer GCN is then given as follows where  $Z$  refers to the embedding or output of the target node (Kipf & Welling 2016, p. 3):

$$Z = f(X, A) = \text{softmax} \left( \hat{A} \text{ReLU} \left( \hat{A} X W^{(0)} \right) W^{(1)} \right) \quad (2.24)$$

Finally, the model parameters are updated analogues to the procedure outlined in algorithm 3. The main distinctive feature for the GCN is the differing forward propagation function.

### 2.2.2.2 GraphSage

This section introduces GraphSage by Hamilton et al. (2017) which can be thought of as the inductive counterpart of the GCN presented in the previous section. Inductive refers to the capability of not only performing ML tasks on the graph used for training but to apply the trained GNN model to new and unseen graphs. This is a large leap as GCNs for instance can only be used to predict unseen nodes on the graph which was used for training. This is very limiting for the application of GCNs in a practical setting. GraphSage overcomes this problem by applying different aggregation strategies and sampling the neighborhood  $\mathcal{N}(v)$ . Specifically, the GraphSage model only considers a fixed number of uniformly random sampled neighbors from  $\mathcal{N}(v)$  with depth  $K$ . A typical example of this procedure is shown in figure 2.5:

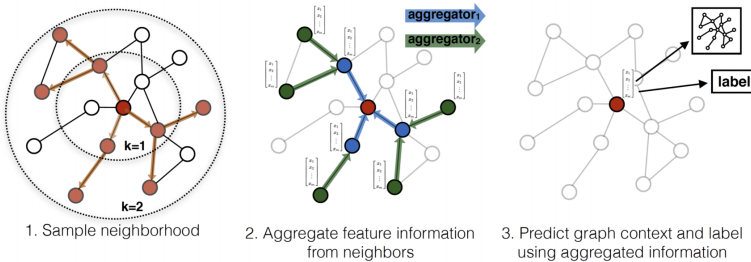


Figure 2.5: GraphSage Sampling  
(Hamilton et al. 2017, p. 2)

The steps shown in figure 2.5 are similar to the procedures for GCNs. The pseudo code for the GraphSage forward propagation function is given in algorithm 4 (Hamilton et al. 2017, p. 12).

Note, that algorithm 4 assumes that the parameters of the aggregator functions and the weight matrices  $W$  are known. Algorithm 4 thus shows the forward propagation of a trained GraphSage model. The model is trained by optimizing the model parameters using mini-batch training for a specified number of epochs. The training procedure can be implemented by using an adaptation of the general procedure

**Algorithm 4:** GraphSage Mini-batch Forward Propagation Algorithm

---

**Input:** Graph  $G(V, E)$ ;  
     input features  $\{x_v, \forall v \in \mathcal{B}\}$ ;  
     depth  $K$ ;  
     weight matrices  $W^k, \forall k \in \{1, \dots, K\}$ ;  
     non-linearity  $\sigma$ ;  
     differentiable aggregator functions  $AGGREGATE_k, \forall k \in \{1, \dots, K\}$ ;  
     neighborhood sampling functions,  $\mathcal{N}_k : v \rightarrow 2^v, \forall k \in \{1, \dots, K\}$

**Output:** Vector representations  $z_v$  for all  $v \in \mathcal{B}$

```

1  $\mathcal{B}^K \in \mathcal{B}$ 
2 for  $k = K \dots 1$  do
3    $\mathcal{B}^{k-1} \leftarrow \mathcal{B}^k$ 
4   for  $u \in \mathcal{B}^k$  do
5      $\mathcal{B}^{k-1} \leftarrow \mathcal{B}^{k-1} \cup \mathcal{N}_k(u)$ 
6   end
7    $h_u^0 \leftarrow x_v, \forall v \in \mathcal{B}^0$ 
8   for  $k = 1 \dots K$  do
9     for  $u \in \mathcal{B}^k$  do
10     $h_{\mathcal{N}(u)}^k \leftarrow AGGREGATE_k(\{h_{u'}^{k-1}, \forall u' \in \mathcal{N}_k(u)\})$ ;
11     $h_u^k \leftarrow \sigma(W^k \cdot CONCAT(h_u^{k-1}, h_{\mathcal{N}(u)}^k))$ ;
12     $h_u^k \leftarrow h_u^k / \|h_u^k\|_2$ 
13   end
14 end
15  $z_v \leftarrow h_u^K, \forall u \in \mathcal{B}$ 

```

---

shown in algorithm 3. Note, that the parameters of the aggregation functions and the weight matrices  $W$  are all layer specific elements of  $\Theta$  in algorithm 3. For algorithm 4,  $\mathcal{B}$  refers to the mini-batches of vertices taken from the set of vertices  $V$  of the graph  $G(V, E)$ .

There are three aggregator strategies proposed for GraphSage by Hamilton et al. (2017, p. 5-6). In addition, sum-pooling is added as a fourth strategy and is listed with the other three aggregation approaches as follows:

1. Mean aggregation
2. Max-pooling
3. Long short-term memory (LSTM) aggregation
4. Sum-pooling

The four proposed aggregation strategies are briefly introduced in the following paragraphs:

### Mean Aggregation

This type of aggregation is similar to the GCN and takes the average of the received messages from the message passing procedure. The difference to the GCN is that mean aggregation does not require the full graph Laplacian and makes use of a slightly different normalization approach. The aggregation process differs to the one

shown in algorithm 4 and replaces the procedures in line 9 and 10 with (Hamilton et al. 2017, p. 5):

$$h_v^k \leftarrow \sigma(W \cdot \text{MEAN}(\{h_v^{k-1}\} \cup \{h_u^{k-1}, \forall u \in \mathcal{N}(v)\})) \quad (2.25)$$

### Max-Pooling Aggregation

Max-Pooling aggregation refers to the application of an element-wise max operator. This means that of the neighbors, only the largest element-wise features are considered. More formally, max-pooling aggregation is defined as follows and is used for the aggregation shown in line 9 of algorithm 4 (Hamilton et al. 2017, p. 6):

$$\text{AGGREGATE}_k^{\text{pool}} = \max(\sigma(\{W_{\text{pool}} h_{u_i}^k + b, \forall u_i \in \mathcal{N}(v)\})) \quad (2.26)$$

Note, that  $W_{\text{pool}}$  refers to a separate weight matrix for the one layer message passing of the max-pooling aggregation. In principle, an arbitrary number of layers could be added for max-pooling. The authors (Hamilton et al. 2017, p. 6) however focus on the case with one layer. This approach is kept as it yielded good results. The parameters of max-pooling are learned analogues to the other GraphSage model parameters.

### LSTM Aggregation

Long short-term memory (LSTM) is the last aggregation strategy proposed for GraphSage and uses the LSTM recurrent neural network (RNN) first introduced by Hochreiter & Schmidhuber (1997) as an aggregation strategy. LSTMs are not permutation invariant which is a requirement for the aggregation strategy. The authors propose using a random permutation of the set of node neighbors to counter this problem (Hamilton et al. 2017, p. 5). The LSTM parameters are trained along with the other GraphSage model parameters.

### Sum-Pooling Aggregation

The sum-pooling applied in the GraphSage model follows the same procedure as max-pooling. The only difference is that element-wise sum-pooling is performed instead of element-wise max-pooling. Xu et al. (2019) show that certain graph structures can confuse aggregation strategies such as mean aggregation or max-pooling. The issue with these aggregation strategies is, that they are not injective functions. Different input nodes (with different graph structures) in a mean- or max aggregation setting can yield an identical output. Given an identical output, the GNN would classify the two identical outputs as the same node representation even though they are the result of different graph structures. This is an area where

GNNs can fail to distinguish graph structures. Examples of where sum aggregation succeeds and mean- and/or max aggregation fails is shown in figure 2.6:

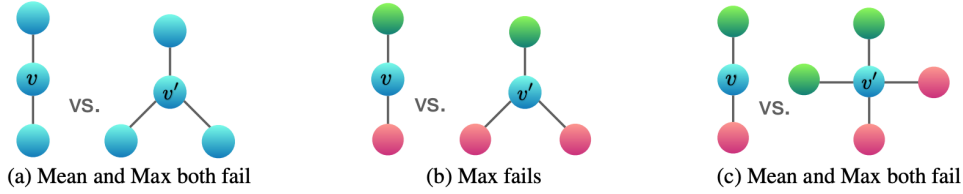


Figure 2.6: Examples of Graph Structures that Mean and Max Aggregators Fail to Distinguish.

(Xu et al. 2019, p. 6)

The node coloring shown in figure 2.6 corresponds to the one-hot encoded types of nodes. Further,  $v$  and  $v'$  should correspond to different node representations, which mean- and/or max aggregation fail to distinguish from each other (hence the same node coloring). Given one-hot encoded nodes with no feature data, sum aggregation is shown to be an injective function (Xu et al. 2019, p. 5). The datasets considered in this thesis contain many features. For that reason, sum-pooling alone is unfortunately not an injective function. The potential advantages of sum-pooling nevertheless sparked the interest in this aggregation strategy. For that reason, sum-pooling is added as an aggregation strategy of interest for the GraphSage model.

## 2.3 Graph Generation

This section introduces the multiplicative attribute graph (MAG) model by Kim & Leskovec (2012). This model is used to generate semi-synthetic graphs from feature data as mentioned in the introduction. Originally, the MAG model was introduced for the purpose of generating realistic graphs from feature data and to show that the resulting graph can obey properties of real-world networks. To show this, Kim & Leskovec generated random feature data for which the model parameters were set in such a manner, that the resulting graph adheres to a set of real network properties. These network properties include the emergence of a giant connected component and a power-law or log-normal degree distribution among others (Kim & Leskovec 2012, p. 113). While the creation of a graph which follows real-world network properties would be desirable, it is not the primary target for this thesis. The main goal of the semi-synthetic graph generation is to create a graph that provides useful additional information, which can be exploited using GML. The MAG model is flexible in this sense, that it can create graphs which are not constrained to adhere to a specific set of network properties. Lastly, Kim & Leskovec (2012, p. 138-139) present model parameters which generate graphs that follow real-world network properties. These

model parameters can however not be adopted for the task at hand. The parameters were created for a somewhat simpler task which "only" involved randomly generated feature data. These randomly generated features do not correspond to any specific features. For that reason, the model parameters can be chosen freely such that the generated network follows real world network properties. The aim of Kim & Leskovec was primarily to create random graphs that can adhere to said network properties. For this thesis, the same MAG model will be applied using real feature data. This makes the task of defining the model parameters more difficult as they cannot be freely assigned. In addition, the generated graph will be used for ML which is not an application the authors had considered. In this regard the reason and aim for using the MAG model differs for this thesis compared to the original paper.

The starting point of the MAG model is a matrix of feature data,  $X^{N \times F}$ , where  $N$  refers to the number of observations and  $F$  to the number of features. Kim & Leskovec refer to feature data as attributes and they use the terms interchangeably. For this thesis a distinction is made, where features correspond to the full set of feature data and attributes refer to the  $K$  number of features used for generating the graph,  $G(V, E)$ . The attribute data,  $B^{N \times K} \subseteq X^{N \times F}$ , is therefore a subset of the feature data. As a selection criterion, attribute data must be of such a manner that reasonable link-affinity matrices,  $\Theta_i$ , can be defined. In addition, attribute data must be discrete. For practical reasons, the cardinality of the attributes should not be too large. Attributes such as age might have to be discretized into 4 or 5 discrete age categories. The link-affinity matrix  $\Theta_i$  is a matrix containing probabilities which are used to estimate the probability of two observations in the dataset  $(u, v)$  to form a connection. More specifically, the probability for a connection is calculated given the attributes  $a_i$  of observation  $u$  and  $v$  where  $(a_i(u), a_i(v)) \in B$ . For example, a reasonable assumption could be to assume, that people which are of the same age group are more likely to be similar and thus form a connection compared to people which are not of the same age group. Another example for this could be gender in terms of biological sex which is a classical binary setting for a link-affinity matrix. Examples of binary attribute link-affinity matrices  $\Theta_i$  are given in figure 2.7.

Figure 2.7 shows 4 types of link-affinity matrices depending on the type of relationship one wants to model. Homophily refers to love of the same which would make a connection between two observations more likely if they have the same attributes. Similarly, Heterophily refers to the love of the different where observations which do not have the same attributes are more likely form a connection. Core-periphery is a special case which can be used to generate realistic social-networks in terms of network properties (Kim & Leskovec 2012, p. 139). As an example, an attribute

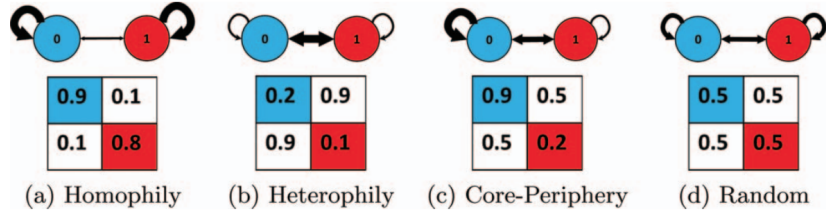


Figure 2.7: Attribute Link-Affinities  
(Kim & Leskovec 2012, p. 118)

could indicate whether a person is a member of the local football club. In a core-periphery setting, members of the local football club are very likely to be connected, while non-members have a significantly lower probability of forming a connection. Lastly, random graphs can be generated by setting the link-affinity probabilities to 0.5. Given the type of attributes available in the data sets, graphs will be generated using homophily structures. The attribute link-affinity matrices  $\Theta_i$  are defined for every attribute and can be set for an arbitrary size of categories within an attribute. More formally for each observation  $u \in B$  with  $K$  categorical attributes of cardinality  $d_i$  for  $i = 1, 2, \dots, K$  and corresponding link-affinity matrices  $\Theta_i^{d_i \times d_i}$  for  $i = 1, 2, \dots, K$ , the probability  $P[u, v]$  of a connection between observations  $(u, v)$  is defined as (Kim & Leskovec 2012, p. 119):

$$P[u, v] = \prod_{i=1}^K \Theta_i [a_i(u), a_i(v)] \quad (2.27)$$

In equation 2.27,  $a_i(u)$  refers to the value of the  $i$ th attribute of observation  $u$ . A schematic representation of the procedure for a binary link-affinity matrix is shown in figure 2.8.

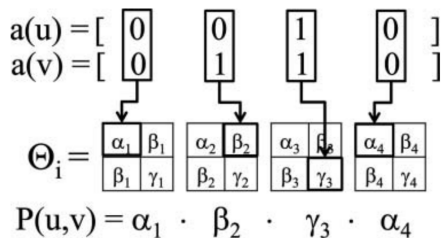


Figure 2.8: Schematic Representation of the Multiplicative Attribute Graphs (MAG) Model

(Kim & Leskovec 2012, p. 120)

The pseudo-code of the MAG model is depicted in algorithm 5 and generates the adjacency matrix  $A$  which is then used for constructing the graph  $G(V, E)$ . The observations of the feature data  $X$  which contains the attributes are used as inputs

**Algorithm 5:** Multiplicative Attribute Graph Model

---

**Input:** graph node-attribute generation matrix  $B^{N \times K}$ , where  $B \subseteq X^{N \times F}$ ;  
node attribute vector  $a_i$  with cardinalities  $d_i$  for  $i = 1, 2, \dots, K$ ;  
link affinity matrices  $\Theta_i^{d_i \times d_i}$ , for  $i = 1, 2, \dots, K$ ;

**Output:** adjacency Matrix  $A^{N \times N}$  for Graph  $G(V, E)$

```

1   $B^{K \times N} = B^T$ 
2  for  $j = 1, 2, \dots, N$  do
3     $u = B[:, j]$ 
4    for  $k = 1, 2, \dots, N$  do
5       $v = B[:, k]$ 
6      for  $i = 1, 2, \dots, K$  do
7         $P_{j,k} = \prod_{i=1}^K \Theta_i[a_i(u), a_i(v)]$ 
8    end
9  end
10  $U^{N \times N} = \text{uppertriangular}(P)$  with  $\text{diag}(U) = 0$ 
11 for  $i = 1, 2, \dots, N$  do
12   for  $j = 1, 2, \dots, N$  do
13     if  $U_{i,j} > \mathcal{U}(0, 1)$  then
14        $\hat{A}_{i,j} = 1$ 
15     else
16        $\hat{A}_{i,j} = 0$ 
17     end
18   end
19 end
20  $A = \hat{A} + \hat{A}^T$ 

```

---

and correspond to the nodes in the resulting graph. More precisely, the order of the generated adjacency matrix  $A$ , corresponds to the ordering of the feature matrix  $X$ . Therefore, the features can be assigned to the nodes of the generated graph. The procedure outlined in algorithm 5 can be summarized with the following sequential steps:

1. Calculate the connection probabilities  $P$  between every observation in the attribute matrix  $B$  using equation 2.27.
2. As only undirected graphs are considered, the upper triangular matrix  $U$  of  $P$  is taken where the  $\text{diag}(U) = 0$ . The diagonal of  $U$  is set to 0 to exclude self-loops.
3. For every element in  $U$ , draw a random number from a standard uniform distribution  $\mathcal{U}(0, 1)$ . If the connection probability  $P_{u,v} > \mathcal{U}(0, 1)$ , a 1 in the preliminary adjacency matrix  $\hat{A}_{u,v}$  is recorded. Otherwise a 0 is recorded.
4. The preliminary adjacency matrix  $\hat{A}$  is an upper triangular matrix with  $\text{diag}(\hat{A}) = 0$  and all elements in the lower triangular also being equal to 0. As the target is to create an undirected graph, the corresponding adjacency matrix is symmetric which is why the final adjacency matrix can be created using  $A = \hat{A} + \hat{A}^T$ .

# Chapter 3

## Data

This chapter introduces the datasets used for this thesis. Several approaches and datasets were considered for evaluating the success of GML on semi-synthetic graphs. In particular, three datasets were considered with varying degrees of success which are:

1. Self launched survey
2. Bank telemarketing dataset
3. US airline passenger dataset

The datasets are introduced to the extent that they are successful or useful within the framework of this thesis. In particular, the self launched survey and the bank telemarketing dataset showed to be problematic for different reasons. They however provide valuable insights as to when GML can be successful. These two datasets are therefore only briefly introduced with the focus lying on providing the relevant insights gained from these "failed" datasets. The detailed introduction and analysis of these datasets is therefore skipped. The data and the analyses of these two datasets are provided in the GitHub repository referenced in section 3.1. The US airline passenger satisfaction dataset is presented in detail, as good results are achieved using GML. In addition, good results were also achieved for this dataset using standard ML models. For that reason, the US airline passenger dataset will be used for comparing the results of GML and standard ML in chapter 4.

Before introducing the datasets, the programming language and the packages used for the analyses are thankfully referenced in the following section. In addition, the GitHub repository containing the datasets and the python code is referenced.

## 3.1 Software & Code

The entire master’s thesis was evaluated using the Python 3.8.10 programming language (Van Rossum & Drake 2009). In addition, following open-source python packages were thankfully used which are Numpy 1.20.2 (Harris et al. 2020), Matplotlib 3.3.4 (Hunter 2007), NetworkX 2.5.1 (Hagberg et al. 2008), Seaborn 0.11.1 (Waskom 2021), Pandas 1.2.5 (McKinney et al. 2010), Statsmodels 0.12.2 (Seabold & Perktold 2010), Scikit-Learn 0.24.2 (Pedregosa et al. 2011), Tensorflow 2.4.0 (Abadi et al. 2016), Pytorch 1.7.0 (Paszke et al. 2019), deep graph library (dgl) 0.6.1 (Wang et al. 2019), tqdm 4.61.1 (da Costa-Luis et al. 2021) and Node2Vec 0.4.3 (Cohen 2021).

The datasets as well as the Python code used for creating and analyzing the data can be found in a public GitHub repository<sup>1</sup>. The GitHub repository also includes the Python code for the results shown in chapter 4. The repository serves as a general reference for the datasets and the Python code used for this thesis. For every folder in the GitHub repository, there is a readme file which describes the files present in the corresponding folder. In addition, the Python code is written in Jupyter Notebooks which include descriptions of the code. Last but not least, the implementation of the GraphSage model is partially derived from a tutorial given at the KDD (2020) conference.

## 3.2 Self Launched Survey

Initially, the aim for this master’s thesis was to make use of a self launched survey which focused on a bank client classification task. The classification task was two-fold in that a simpler task focused on classifying bank clients as to whether they would be interested in investing or not. The second classification task involved classifying clients according to their investment preferences in terms of products (single securities like stocks or bonds, funds, ETFs, etc.). The attributes used for creating the MAG included mostly demographic data. Additional data was collected which assessed the financial knowledge and behavioral profile of the survey participants by using questions from the financial literacy report of the OECD (2017). The idea was, that demographic data coupled with the financial literacy questions should provide a suitable database for the given bank client classification task.

Unfortunately, only  $n = 113$  people participated in the survey which in general is very small for a ML task. Further, the graphs generated using the MAG method

---

<sup>1</sup>GitHub repository: <https://github.com/MichaelvonSiebenthal/MasterThesis.git>

were not stable. Due to the stochastic characteristic of the MAG model, the resulting graphs could differ dramatically. This lead to significant performance differences for the different ML methods applied to the resulting graphs. Classification accuracies ranged between 40 - 95%. A remedy for this problem could be to assign a fixed probability threshold such as 0.5 in the MAG model. With a fixed threshold probability, the MAG model would generate deterministic graphs which are always the same. The downside however is, that this makes the graph generation process less realistic. In a homophily setting this would assume, that a connection is formed with any node where  $P[u, v] > 0.5$ . It is unclear without testing, what impact this would have on the graph generation process and whether it would have a positive or a negative impact for GML. It is well understood, that people often form connections with people that appear unlikely from a probabilistic perspective. This consideration would warrant the generation of stochastic graphs. The main priority is however to create graphs which provide additional information that can be exploited via GML. Having this objective in mind, it warrants further investigation for which the results are presented in section 3.4.2.

The self-launched survey could not be used for any meaningful analysis due to the small sample size. Nevertheless, it provided an interesting follow-up question regarding the generating of stochastic vs. deterministic graphs. The dataset was discarded for further analysis and the survey data as well as the performed analyses can be found in the GitHub repository.

### 3.3 Bank Telemarketing Dataset

The bank telemarketing dataset first introduced by Moro et al. (2011, 2014) was considered as a banking related backup dataset for the case that the self made survey did not yield a sufficient number of responses. The bank telemarketing dataset is based on a marketing campaign at a Portuguese bank. The dataset includes demographic data, data regarding the bank client's wealth, contact success during previous campaigns among others. The dataset further provides the label data which indicates whether a client invested in a short-term deposit after having been contacted by the call center of the bank. The dataset is therefore set up for a binary classification task. The MAG generated from the bank telemarketing dataset is shown in figure 3.1.

The red dots in figure 3.1 mark the clients which decided to invest in the short-term deposit and the blue dots did not invest. This figure masks some of the blue nodes due to the figure generation process. The general pattern however is apparent. The red nodes are randomly placed in the network which suggests, that

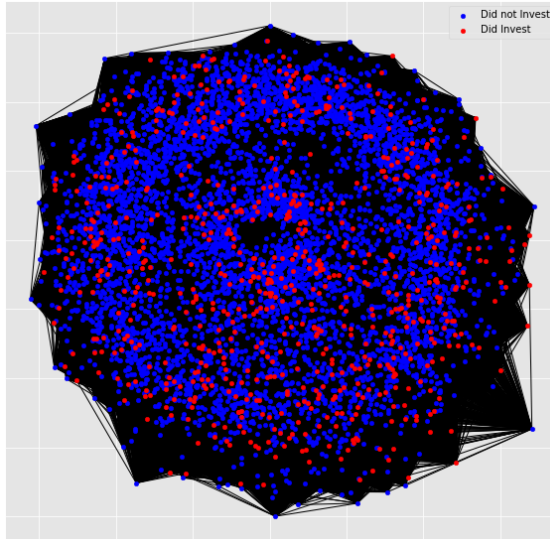


Figure 3.1: MAG of Bank Telemarketing Dataset

GML will be of limited use. The graph further shows, that only a relatively small number of clients appear to have invested in the short-term deposit. To be more precise, only approximately 12% of bank clients invested in the short-term deposit. The dataset is unbalanced which makes the classification task difficult. GRL using Node2Vec fails to overcome the challenge set by the unbalanced nature of the dataset as shown in appendix B.1. The results using GNNs also perform rather poorly. In particular, GNNs tend to classify most clients as non-investors and struggle to accurately classify clients which did invest. Due to the unbalanced data, it is loss optimizing for the GNNs to predict most nodes as non-investors rather than learning the true label. Table 3.1 shows the confusion matrix of the classification results for the validation dataset (20%) of the GraphSage model. This model yielded the best results among all GNN models.

Predicted Label \	Did not invest	Invested
Did not invest	1'000	55
Invested	104	54

Table 3.1: Confusion Matrix Validation Bank Telemarketing Data

The confusion matrix corresponds to an accuracy of approximately 86.89%. The MAG generation process was repeated multiple times for which the GraphSage accuracies ranged between 86 - 90%. Similar results were achieved for both graph based methods and standard ML models such as ANNs, SVMs, and random forest classifiers. The results for these standard ML models are shown in appendix C.1.

Unbalanced datasets are part of a larger and common problem in ML. Possible reme-

dies might include using loss functions which penalize false classifications harsher than the standard cross-entropy loss function used for the GNNs. Alternatively, one could also reduce the dataset by dropping observations so that the remaining dataset is balanced. This approach has its own problems as dropping a large number of observations discards a lot of potentially valuable information. It could also put in question the external validity of the model. These comments point to a separate field of research and could be interesting for a future project.

The failure using GML models for this dataset reveals, that GMLs are not an easy remedy for unbalanced data. Perhaps, if the network structure provided clusters which corresponded to the labels, GMLs could provide superior results. Given the variables available in the dataset and the limitations of using the MAG model, this is not possible. In order to check, whether network structure could indeed remedy the unbalanced label problem, the label of the bank telemarketing dataset was used as an additional attribute for the MAG model. The label is normally not included as an attribute for the MAG model, as the label data is usually unknown outside of the training dataset. The link-affinity probabilities for the label is set as follows:

$$\Theta_{label} = \begin{pmatrix} 0.95 & 0.25 \\ 0.25 & 0.95 \end{pmatrix}$$

The resulting MAG which considers the label as an attribute is shown in figure 3.2.

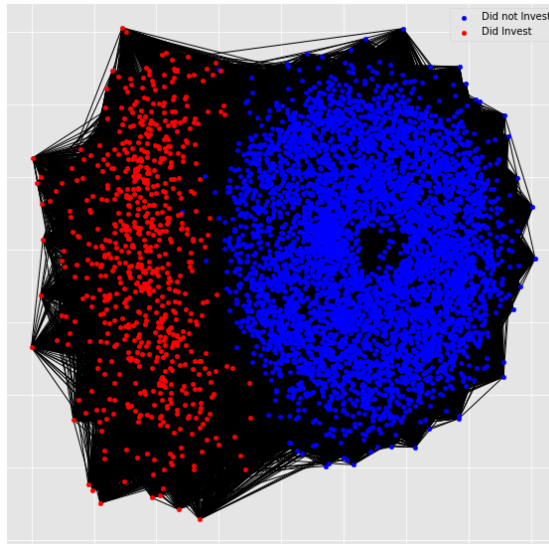


Figure 3.2: Biased MAG of the Bank Telemarketing Dataset

The nodes shown in figure 3.2 are now nicely clustered according to their label. The GNN model GraphSage achieved an accuracy of over 95% for this graph using otherwise identical feature data and model specifications as before. This is of course a form of cheating, as one cannot assume to know the labels of the graph outside of

the training setting. In a real-world application, the model would be trained using label data and then applied to new data which does not contain the label. This approach would however require the label for the graph generation procedure which makes this not a viable approach. Nevertheless, this result shows extremely well when GML can yield superior results compared to standard ML models. The key lies in generating a graph with a network structure that corresponds to the label. The network structure need not necessarily be as clearly separated as shown in figure 3.2. A graph which contains local neighborhood clusters which correspond to the same label could yield similar good results. In such a setting, one would have to be careful when defining the number of  $K$  layers and the neighborhood sampling function  $\mathcal{N}_k$ . A network structure which corresponds to the label could perhaps also be generated without the label to an extent. This would require that the attribute data used in the MAG model to be related with the label. The attributes would have to be substitutes for generating a network structure which correspond to the label. Given the available attributes for the bank telemarketing dataset, this is a difficult task. All features in the dataset have very low correlations with the label. The largest correlation, which is a strong outlier, with the label is call duration with a correlation coefficient  $r \approx 0.4$ . This value is rather small and a simulation showed, that it could not be used as a single substitute for the label. Selecting the appropriate attributes and defining the link-affinity probabilities is not a trivial task and requires a lot of trial and error. Unfortunately, for this dataset no appropriate attributes and link-affinities were found that yielded the desired result. For that reason, this dataset was also discarded for further analysis. The dataset and the performed analyses can be found in the GitHub repository.

## 3.4 US Airline Passenger Dataset

The US airline passenger dataset is a survey which was conducted in 2015 by J.D. Power (2015). The dataset was retrieved on the website Kaggle (2020) and is well suited for applying GML following the MAG generation procedure. The dataset focuses on classifying satisfied- and neutral or dissatisfied passengers. The dataset is thus set up for a standard binary classification task. The dataset further proves to be a competitive dataset for standard ML models. This makes this dataset a suitable candidate for a fair comparison of GML vs. standard ML. This dataset is presented in detail as it is used for the results shown in chapter 4.

An overview of the US airline passenger dataset is shown in table 3.2. The correlation heatmap of the dataset is further shown in figure 3.3. The correlation heatmap reveals, that the variables "departure delay in minutes" and "arrival delay

in minutes" are highly correlated. As "arrival delay in minutes" has some missing observations, this variable is dropped in favor of "departure delay in minutes". The heatmap and its corresponding correlation matrix reveal, that "gender" is approximately uncorrelated with any of the other variables. Further, "departure delay in minutes" appears to be approximately uncorrelated with any of the other variables. For that reason, it was tested whether both variables could be excluded. The results however reveal, that the ML models performed better if these variables are included in the model. The data shown in table 3.2 and figure 3.3 corresponds to a random sample of 6'000 observations from the training dataset consisting of 103'904 observations. The training graph is created using this sample of 6'000 observations due to computational time considerations. Several random samples were used to generate MAGs, for which the results of all simulations were consistent.

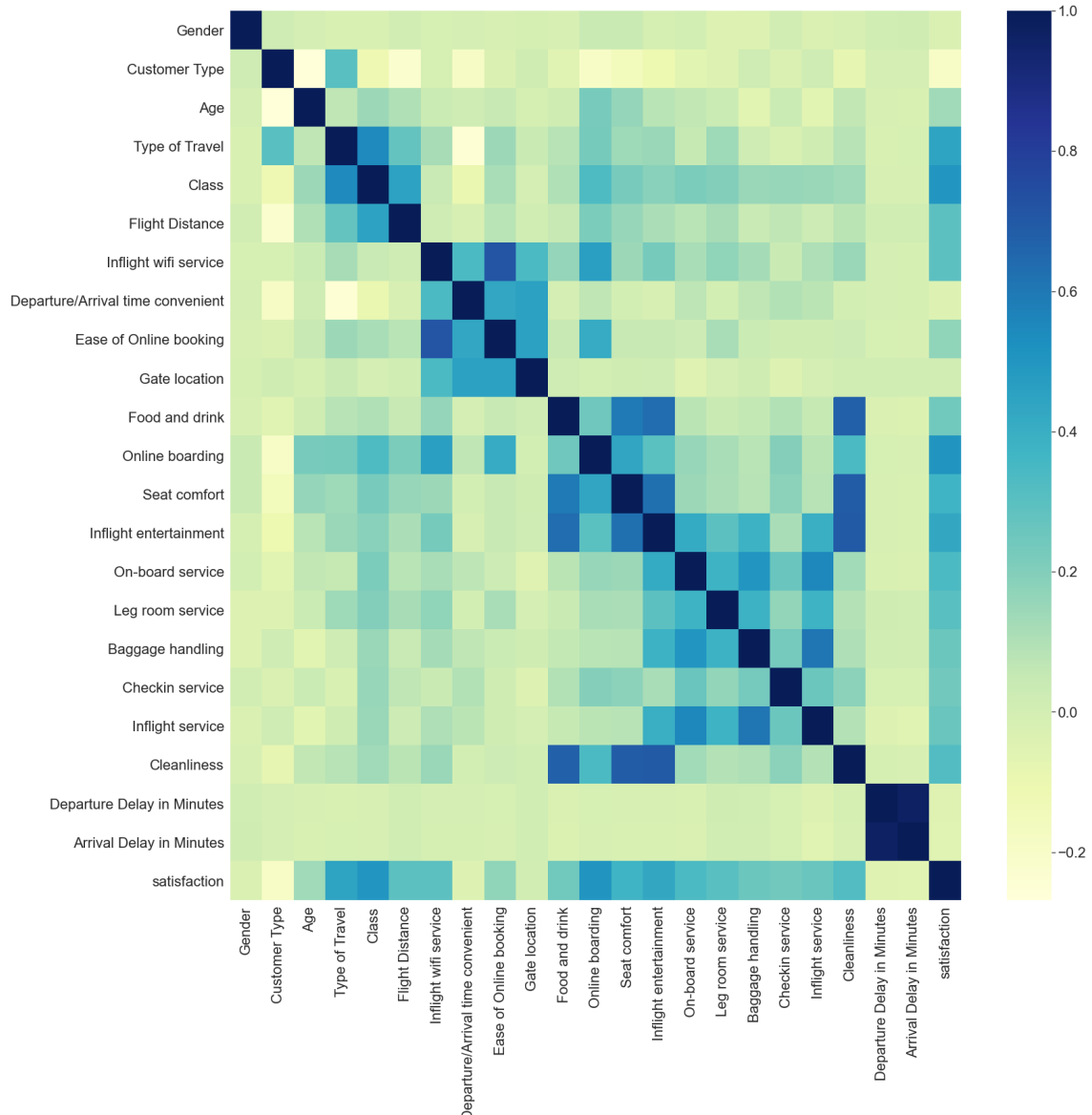


Figure 3.3: Correlation Heatmap of US Airline Passenger Dataset

<b>Variable</b>	<b>Description</b>	<b>Mean</b>	<b>Range</b>
Satisfaction (label)	Satisfaction: Airline satisfaction level (satisfied:1, neutral or dissatisfied:0)	0.4295	0 - 1
Gender	Gender of the passengers (male:0, female:1)	0.5076	0 - 1
Customer Type	The customer type (loyal customer:0, disloyal customer:1)	0.18	0 - 1
Age	The actual age of the passengers	39.101	7 - 85
Type of Travel	Purpose of the flight of the passengers (personal travel:0, business travel:1)	0.6891	0 - 1
Flight Distance	The flight distance of this journey	1'197.438	67 - 4'963
Departure Delay in Minutes	Minutes delayed when departure	14.808	0 - 595
Arrival Delay in Minutes	Minutes delayed when arrival	15.159	0 - 589
Class	Travel class in the plane of the passengers (Eco:1, Eco Plus:2, Business:3)	-	1 - 3
Inflight WiFi service	Satisfaction level of the inflight WiFi service (0:not applicable;1-5)	-	0 - 5
Ease of Online booking	Satisfaction level of online booking	-	0 - 5
Gate location	Satisfaction level of gate location	-	0 - 5
Food and drink	Satisfaction level of Food and drink	-	0 - 5
Online boarding	Satisfaction level of online boarding	-	0 - 5
Seat comfort	Satisfaction level of seat comfort	-	0 - 5
Inflight entertainment	Satisfaction level of inflight entertainment	-	0 - 5
On-board service	Satisfaction level of on-board service	-	0 - 5
Leg room service	Satisfaction level of leg room service	-	0 - 5
Baggage handling	Satisfaction level of baggage handling	-	0 - 5
Check-in service	Satisfaction level of check-in service	-	0 - 5
Inflight service	Satisfaction level of inflight service	-	0 - 5
Cleanliness	Satisfaction level of cleanliness	-	0 - 5

Table 3.2: US Airline Passenger Dataset

The variables of the dataset are categorized as follows:

- **Categorical Variables:** gender, customer type, type of travel, and satisfaction
- **Ordinal Variables:** class, inflight wifi service, ease of online booking, gate location, food and drink, online boarding, seat comfort, inflight entertainment, on-board Service, leg room service, baggage handling, check-in service, inflight service, and cleanliness
- **Numerical Variables:** age, flight distance, and departure delay in minutes

The categorical variables are dummy coded and the ordinal variable class is coded as shown in table 3.2. The remaining ordinal variables which measure different satisfaction levels are recorded using a Likert scale ranging from 1 – 5. Many passengers did not answer all satisfaction level questions. These responses are recorded with a 0. Therefore, the range of values for the satisfaction level variables range from 0 – 5. This encoding works well, as a 0 input in a linear pass function of a (graph) neural network will result in a 0 output value. This type of encoding allows for dealing with missing values for neural networks and other ML models. Lastly, the numerical variables had to be normalized. The popular approach of standardizing the entire dataset was unfortunately not possible. Due to the missing values prevalent in the satisfaction level variables, it must be ensured, that a 0 refers to as a missing response. Note, that a recorded 0 for the numerical variables does not correspond to a missing value. For that reason, the min-max normalizing function was applied and is defined as follows:

$$x' = a + \frac{(x - \min(x))(b - a)}{\max(x) - \min(x)} \quad (3.1)$$

In equation 3.1,  $x$  refers to the unnormalized variable and  $x'$  refers to resulting normalized variable.  $a$  defines the lower bound of the normalization range and  $b$  is the upper bound. The numerical variables are normalized to be within the range [1, 5]. Now, all variables are within a similar range and different scaling should no longer lead to biasing behavior.

In the following section, the graph generation process for the US airline passenger dataset is described in detail.

### 3.4.1 Graph Generation

To create a graph from the US airline passenger dataset, appropriate attributes must be selected for the MAG model. The selected attributes must be of a type

such that realistic probabilities can be assigned. As an example, it is difficult to assign link-affinity probabilities for people who gave ratings regarding the "inflight wifi service". In this case one could assign a probability that people who gave high ratings are more similar with relative ease. However, does this then also translate to people not liking the wifi-service being similar as well? Further, how do we assign probabilities for people who are dissimilar? These considerations make the selection of appropriate attributes difficult. It is therefore important to select attributes for which realistic probabilities for all of the following three settings can be assigned:

- **Positive similar observations** (e.g. both observations like the service)
- **Negative similar observations** (e.g. both observations dislike the service)
- **Dissimilar observations** (symmetric for undirected graphs, can be asymmetric for directed graphs)

The attributes are selected using the above mentioned considerations. The selected attributes with the corresponding link-affinity probabilities are shown in table 3.3.

Attribute Name	Link-Affinity Probabilities
Gender	0.6, 0.4; 0.4, 0.6
Customer type	0.8, 0.5; 0.5, 0.8
Age	0.90, 0.80, 0.60, 0.40; 0.80, 0.90, 0.80, 0.60; 0.60, 0.80, 0.90, 0.80; 0.40, 0.60, 0.80, 0.90
Type of travel	0.80, 0.20; 0.20, 0.80
Class	0.85, 0.60, 0.45; 0.60, 0.85, 0.60; 0.45, 0.60, 0.85

Table 3.3: Link-Affinity Matrices

The probabilities in table 3.3 correspond to the rows of the link-affinity matrices up to the semi-colon. To give a better overview, the link-affinity matrix for age is shown explicitly as follows:

$$\Theta_{Age} = \begin{pmatrix} 0.90 & 0.80 & 0.60 & 0.40 \\ 0.80 & 0.90 & 0.80 & 0.60 \\ 0.60 & 0.80 & 0.90 & 0.80 \\ 0.40 & 0.60 & 0.80 & 0.90 \end{pmatrix}$$

The attribute age has a rather large cardinality which makes it difficult to use for the MAG model. For that reason, age is binned into 4 categories with 0 if  $age < 26$ , 1 if  $26 \leq age < 39$ , 2 if  $39 \leq age < 50$ , and 3 if  $age \geq 50$ . These bins are chosen according to the interquartile lengths present in the distribution of the attribute age. The transformed attribute now contains 4 categories and now matches the link-affinity matrix shown above.

There exist no clear rules for assigning link-affinity probabilities. Kim & Leskovec (2012, p. 118) presented the 4 common link-affinity matrix structures of homophily, heterophily, core-periphery, and random for creating graphs. Given the selected attribute data, the homophily setting appears to be most appropriate for all link-affinity matrices. In this setting, observations which are similar have a higher probability of forming a connection compared to dissimilar observations. It can however not be ruled out, that different link-affinity matrix structures might be more appropriate. The probabilities shown in table 3.3 were chosen based on personal intuition and trial and error. To test this, several graphs were created using different probabilities. The homophily structure with the probabilities shown in table 3.3 generated the best graphs. There is however no exact science or selection criteria which can be applied for selecting attributes and defining the link-affinity probabilities.

As mentioned in the previous section, a sub-sample of 6'000 observations was retrieved from the training dataset consisting of 103'904 observations. With this random subsample and the attributes shown in table 3.3, the adjacency matrix for the resulting graph  $G(V, E)$  is generated using algorithm 5. The random subsample is retrieved due to the computational cost of running algorithm 5. Simulations which involved creating graphs with different random subsamples show, that the random subsamples are representative for the entire dataset. The generated graph is shown in figure 3.4.

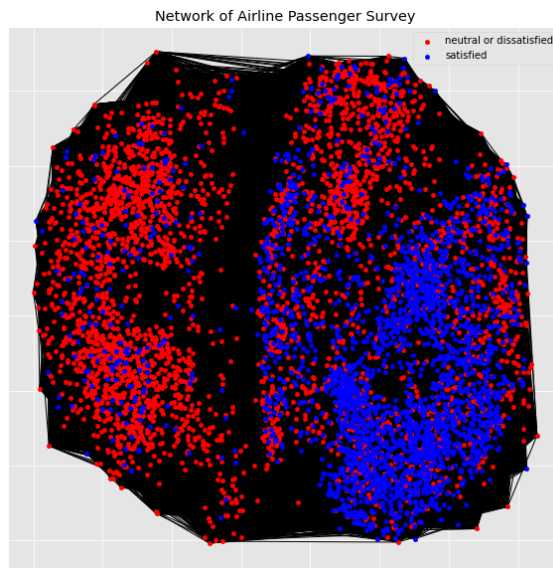


Figure 3.4: Graph of US Airline Passenger Dataset

The network in figure 3.4 shows the emergence of two primary clusters. In addition one can see, that most satisfied airline passengers appear to be grouped together in the right cluster. To gain a deeper understanding of the dynamics involved in

the network formation, the nodes of the network are plotted excluding the edges in figure 3.5.

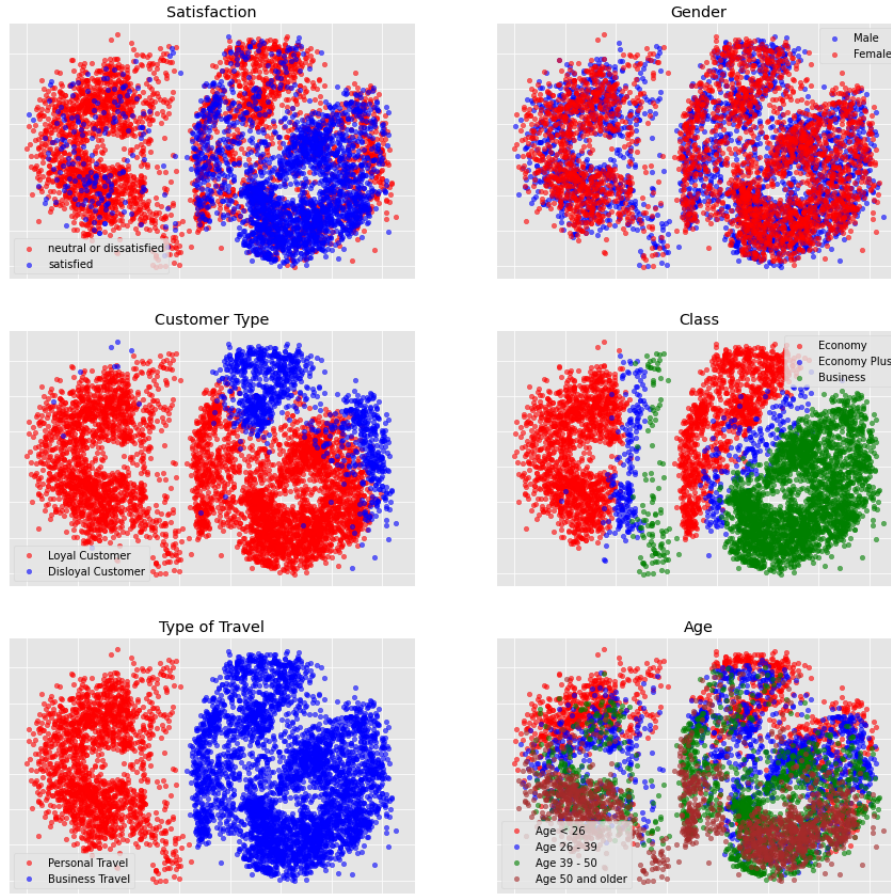


Figure 3.5: Graph Nodes of US Airline Passenger Dataset

Figure 3.5 plots the nodes of the network for the label satisfaction and the 5 attributes used for the graph generation. The transparency of the plot is set to  $\alpha = 0.6$  to avoid covering nodes during the graph plotting process. Figure 3.5 reveals interesting associations. First it is shown, that a larger number of people traveling for business purposes are satisfied compared to people traveling for personal reasons. This association becomes clear when comparing the satisfaction plot with the type of travel plot. In relative terms, only approximately 9.8% of passengers traveling for personal reasons are satisfied compared to business travelers with a 57.8% satisfaction rate. Interestingly, passengers traveling for business purposes adhere to somewhat expected characteristics such as:

1. Most business class passengers are satisfied.
2. Older passengers appear to be more satisfied which is largely associated with booking more business class tickets. The age plot however reveals, that older passengers tend to be mostly satisfied even when booking economy class.

3. Most loyal customers book business class. There is however some overlap where loyal customers also book economy class tickets. The reverse is true as well, where a cluster of disloyal customers book business class.

Passengers traveling for personal reasons do not appear to adhere to the characteristics or associations shown for business travelers. The only distinctive character is, that almost all passenger traveling for personal reasons are loyal customers. This fact does however not appear to be associated with satisfaction. At first, this seems like a rather bizarre finding. Upon further reflection, this could point to a sampling bias of passengers traveling for personal reasons due to following considerations:

1. It is reasonable that almost only loyal passengers participated. When traveling, most people do not participate in surveys. This is especially true for disloyal customers. Business travelers for comparison might give routine feedback due to company policies.
2. It is common, that dissatisfied people are more likely to give feedback, while satisfied passengers are less likely to participate in the survey. Again, the data regarding business travelers might be more reliable here due to company mandated survey participation.
3. Perhaps business travelers fly more frequently than passengers traveling for personal reasons. This could incentivize frequent business travelers to give feedback as they would benefit most from service improvements. Infrequent personal travelers might be less incentivized, as they benefit less from service improvements.

Last but not least, gender does not appear to form any distinguishable clusters. For that reason, it was considered to omit this attribute for the graph generation process. This was tested and the resulting graph was similar to the one shown in figure 3.4. The graph was however more spread out and the neighborhood structures were less clear. In addition, the graph without gender did not perform as well in the subsequent machine learning tasks. Gender appears to provide some useful network information which is why the attribute is kept for the graph generation process.

To provide some more context regarding the graph structure, some graph theoretical metrics are provided. The degree distribution as well as the distributions of the centrality measures: eigenvector centrality, closeness centrality, and betweenness centrality are shown in figure 3.6.

The network has a density of approximately 0.0933. This means that 9% of the potential number of connections formed in the network. Nevertheless, when looking

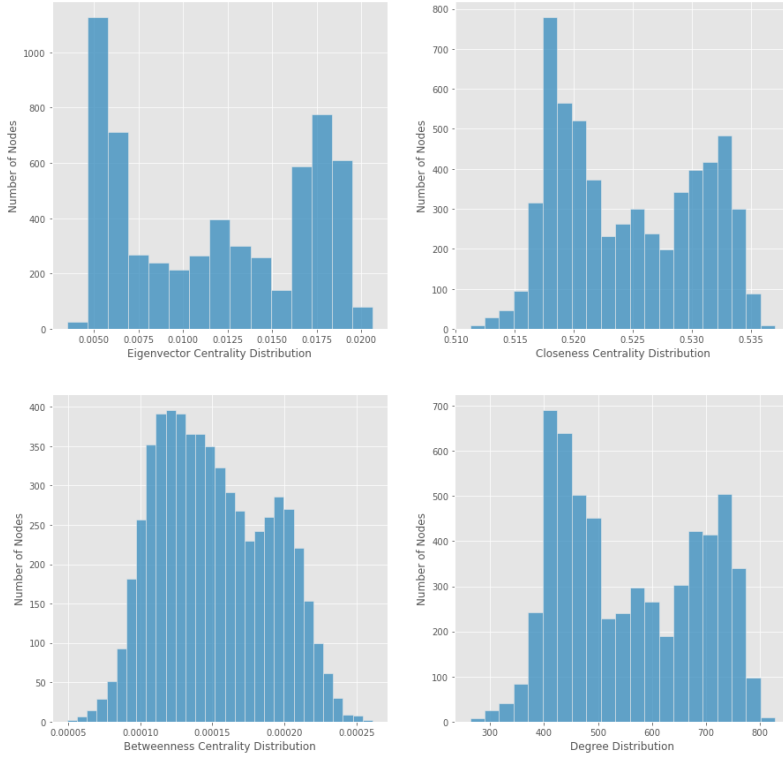


Figure 3.6: Graph Statistics

at the degree distribution histogram we can see, that all nodes have a large number of connections ranging between 263 - 828 with an average of 559.63 connections. The distribution has two modes which likely correspond to the two main clusters shown in figure 3.5. The eigenvector centrality distribution shows, that all nodes have a very low centrality measure and therefore none of the nodes appear to have a large impact in terms of eigenvector centrality. The closeness centrality distribution shows, that all nodes have an average closeness centrality ranging from 0.51 - 0.53. This means that every node is similarly connected and has an average impact for disseminating information across the network. Lastly, the betweenness centrality distribution reveals that there are no bottlenecks through which information flows.

As a reference point, it is important to compare the properties of the created graph to real world graphs. GNNs were designed with real world networks in mind. Especially the large number of vertex degrees might be of concern and is discussed in more detail in section 5.3. For that reason, the generated MAG is compared to real networks. The most appropriate type of networks for comparison are social networks. Common structures of social networks include (Watts & Strogatz 1998, Newman et al. 2006, Newman 2010, Kim & Leskovec 2012):

1. Degree distributions often follow a power law distribution
2. Emergence of a giant connected component

### 3. Core-periphery structure

The power law degree distribution and the emergence of a giant connected component creates network structures that have an onion (core-periphery) structure (Kim & Leskovec 2012, p. 121). This indicates, that most social networks have a few very highly connected nodes and many nodes with few connections. This creates a right skewed degree distribution which also leads to a right skewed eigenvector centrality and closeness centrality distribution. For the betweenness centrality it is also expected, that more central nodes in a core-periphery network structure would exhibit some bottleneck properties for the central nodes. For that reason one would expect central nodes to have a higher betweenness centrality. When looking at the distributions in figure 3.6, this does not correspond to a power law degree distribution. The centrality measures further do not correspond to the centralities frequently observed in real social networks. The graph created with the MAG model does therefore not share the properties observed in real social networks. In order to generate a graph which shares the properties of real networks, one would have to adapt the link-affinity properties to the core-periphery setting as shown in figure 2.7. This was tested and indeed an onion shaped network was created using the same attributes. Forcing this core-periphery structure is however not purposeful for this thesis. This would require setting link-affinity probabilities for the feature data which would not make sense. Further, the aim of this thesis is not necessarily to create realistic graphs rather than to create useful graphs for GML. The results in chapter 4 reveal, that the graph is indeed useful for ML. For that reason, the generated graph shown in this section was kept for further analysis.

#### 3.4.2 Stochastic vs. Deterministic MAGs

In section 3.2, the question was raised as to whether the MAG should form connections between observations stochastically or whether a deterministic threshold probability yields better results. In the previous sections, the graphs were generated stochastically. In this section, the US airline passenger dataset is used for generating a deterministic graph. The first insight gained when investigating this question lies in the fact, that the probability of two observations is generally very low. When setting the threshold probability for a connection between two observations  $u$  and  $v$  to 0.5, not a single connection is made. This follows, as the probability for a connection decreases by design as the number of attributes increases. This is implicitly shown in equation 2.27, where the product of probabilities is bound to approach 0 as the number of attributes increases. For this reason, it is suggested to limit the number of attributes to  $K = \rho \log_2 N$  for some constant  $\rho$  (Kim & Leskovec 2012, p. 122). The number of attributes are selected accordingly such that

$K \leq \log_2 N$ . The threshold probability for a connection was set to 0.2 in the MAG model. The MAG yielded several disconnected graphs which are for the most part clustered according to their group memberships. Figure 3.7 shows the graphs for the label and the attributes, where the edges are removed. The subgraphs are unfortunately plotted very small, however all graphs combined include all 6'000 nodes. The plots are meant to provide a high-level overview of the generated subgraphs.

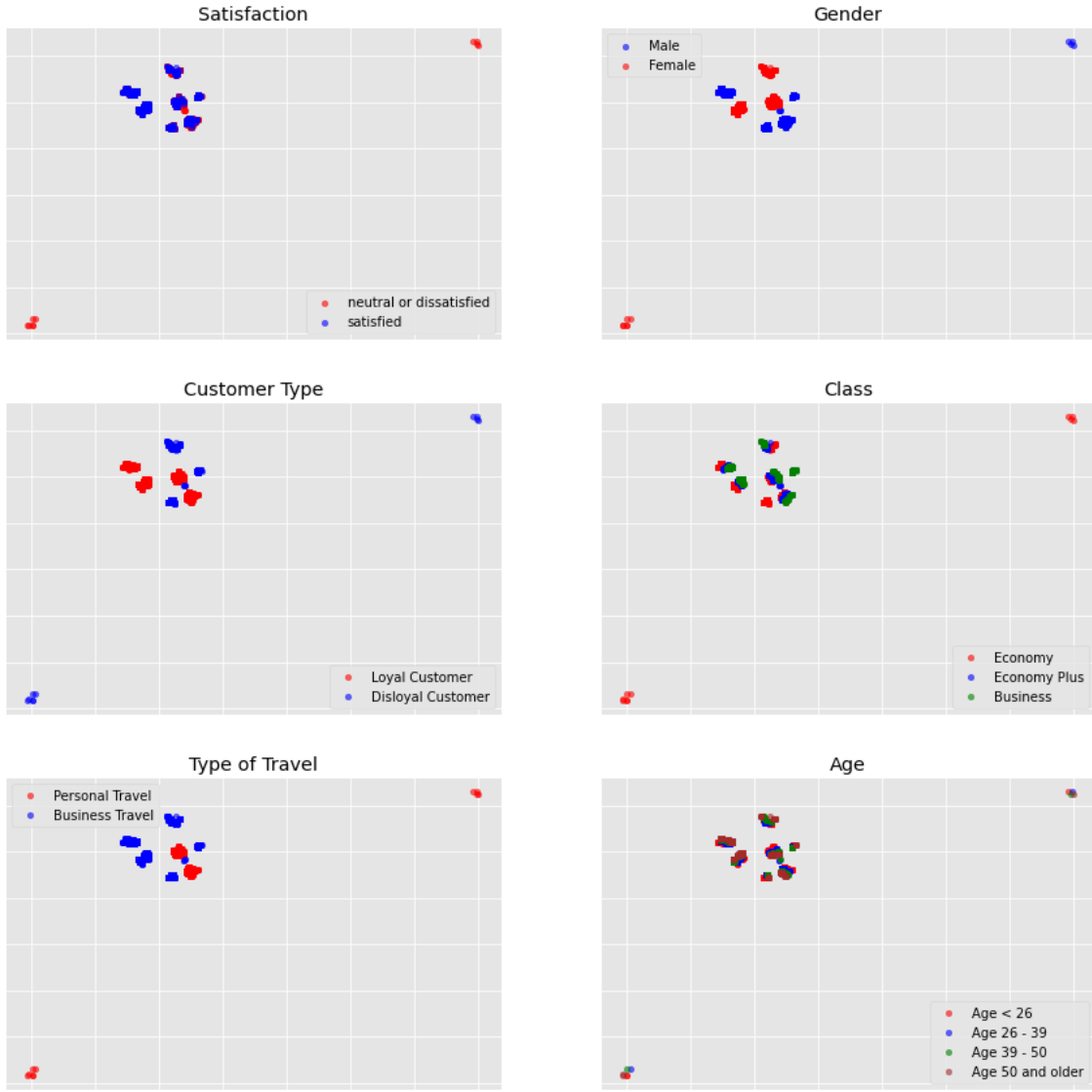


Figure 3.7: Deterministic MAG

The deterministic MAG model creates disconnected graphs which form clusters based on node similarities. In terms of performance, the accuracy and loss behavior of both the deterministic- and stochastic generated graphs were virtually identical. The GML results using GraphSage for the deterministic MAG is shown in appendix C.2. For the purpose of visualization, stochastic graphs are more useful as one can identify the different clusters and their relationships to one another on a single connected graph. For this reason, the stochastic graph generation process is kept.

Nevertheless, deterministic graph generation appears to be useful if one wants to separate nodes into more homogeneous subgraphs. These subgraphs could then be used for subsequent ML tasks with a cluster specific task in mind. The clusters further could provide information as to which clusters tend to be more or less satisfied. This is an area which could be interesting for future research.

# Chapter 4

## Results

This chapter presents the results for the US airline passenger dataset. First, the model specifications and the results using GRL and GNNs are presented. Afterwards, the GML results are compared to the results using standard ML models. For the comparison, the standard models logistic regression (Cramer 2002), naive bayes (Zhang 2004), SVMs (Platt et al. 1999, Chang & Lin 2011), random forest classifiers (Breiman 2001), AdaBoost classifiers (Freund & Schapire 1997, Hastie et al. 2009), QDA (Tharwat 2016), and ANNs (McCulloch & Pitts 1943, Werbos 1974) were considered.

### 4.1 Graph Representation Learning

The graph generated in section 3.4.1 using the MAG model was used for GRL. The Node2Vec algorithm using an unbiased walk was employed for learning the 2-dimensional node representations of the graph. The Node2Vec model specifications were set as follows:

- Embedding size  $d$ : 2
- Random walk length  $t$ : 8
- Number of random walks  $\gamma$ : 100
- Window size  $w$ : 10
- Node batch size: 2
- Return parameter  $p = 1$
- In-out parameter  $q = 1$

With the specified return- and in-out parameters, the Node2Vec output corresponds to the DeepWalk output. The resulting node embeddings are then used as inputs for standard ML models. The node embeddings are shown in figure 4.1.

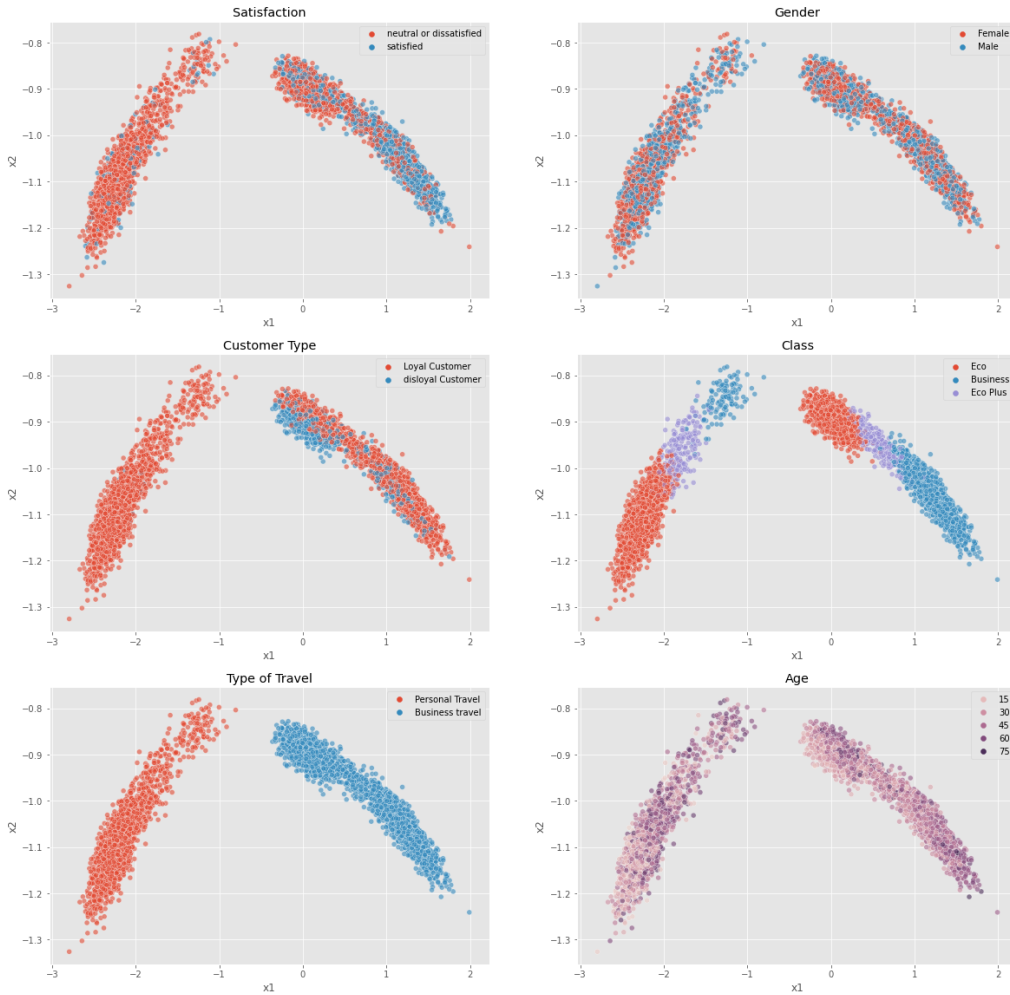


Figure 4.1: Node2Vec Embeddings

The plotted node embeddings in figure 4.1 reveal interesting neighborhood structures. First, the nodes are split according to their type of travel. This corresponds to the two main clusters shown in figure 3.4. Secondly, the node embeddings are grouped in a nice and orderly fashion. The node embeddings are part of Euclidean space, which is why the plots shown in figure 4.1 are proper scatterplots. This allows for a direct comparison of nodes and the groups to which they belong to. The 2-dimensional node embeddings are thus useful for gaining insights via data visualization.

The node embeddings are used as input data for the standard ML models and are shown in table 4.1.

The results show, that the Node2Vec model is not successful for classifying passengers according to their satisfaction. Applying the trained models to the test data yielded even poorer results. When looking at the satisfaction scatter plot in figure 4.1, it becomes obvious why the downstream ML tasks were unsuccessful. Node2Vec

ML Method	Training Accuracy	Validation Accuracy	Test Accuracy
Logistic Regression	77.04%	76.16%	57.05%
Support Vector Machine	76.71%	77.00%	39.08%
ANN	76.78%	78.08%	29.48%
Random Forest	100%	73.08%	40.63%
AdaBoost	76.96%	77.00%	58.22%
Naive Bayes	75.73%	76.43%	56.97%
QDA	75.52%	77.33%	57.00%

Table 4.1: Node2Vec Classification Results

generates very good node embeddings for the attributes to the extent that clusters exist within the original graph. The label satisfaction could not be used as an attribute for generating the graph. This would be unrealistic in practice. As the label is not considered for the graph generation process, Node2Vec does not create embeddings which directly consider the label. The label is only considered to the extent that the attributes create structures which are related with the label. For that reason, the success of any downstream ML method will be limited to the extent that the node embeddings capture relevant information for predicting the label.

Alternative model specifications were tested, which mainly included learning higher dimensional node embeddings. These node embeddings however yielded worse results as shown in appendix B.2. As a final test, the node embeddings were joined to the feature data presented in section 3.4. This data was then used as the input data for the downstream ML models. For the training- and validation data, this approach yielded excellent results with accuracies often being close to 95%. For some of the models such as the random forest classifier, this also translated into a good accuracy for the test data. The results of this approach can also be found in appendix B.2. Unfortunately, the results presented in section 4.3 show, that better accuracies for the test data are achieved by only using the feature data. For that reason, joining feature data with node embeddings is not a recommended approach for the US airline passenger dataset.

## 4.2 Graph Neural Networks

This section presents the results using GNNs. As mentioned in section 2.2.2, the models GCN (Kipf & Welling 2016) and GraphSage (Hamilton et al. 2017) are used for classifying the satisfaction of the US airline passengers. The model specifications and the results are presented in the following sections for both models.

### 4.2.1 Graph Convolutional Networks

The GCN is designed using a similar forward propagation function as the one shown in equation 2.24. The only difference is, that the output layer is activated using the logsoftmax function instead of the softmax function. The outputs of both activation functions are theoretically identical. The logsoftmax function is however numerically more stable, as it internally makes use of the log-sum-exp trick. A good explanation of this trick is given on the website by Gundersen (2020)<sup>1</sup>.

$$Z = f(X, A) = \text{logsoftmax} \left( \hat{A} \text{ReLU} \left( \hat{A} X W^{(0)} \right) W^{(1)} \right) \quad (4.1)$$

The node features  $X$  include the 21 explanatory variables of the US airline passenger dataset as described in section 3.4. The categorical variables are one-hot encoded, which is why the feature matrix includes 24 variables. The hidden layer size of the convolutional layers is also set to 24 and the output layer is set to 2 for the binary classification task. The training loss is calculated using cross-entropy loss and the model parameters are updated using the Adam optimizer (Kingma & Ba 2015) with the learning rate set to 0.002. Essentially, algorithm 3 can be applied by replacing the forward propagation procedure with the function shown in equation 4.1. In addition, the model parameters are updated using the Adam optimizer instead of standard gradient descent. Different model specifications were tested, for which the chosen specifications perform best. The GCN requires approximately 1'000 epochs to finish training. The resulting loss- and accuracy plots are shown in figure 4.2.

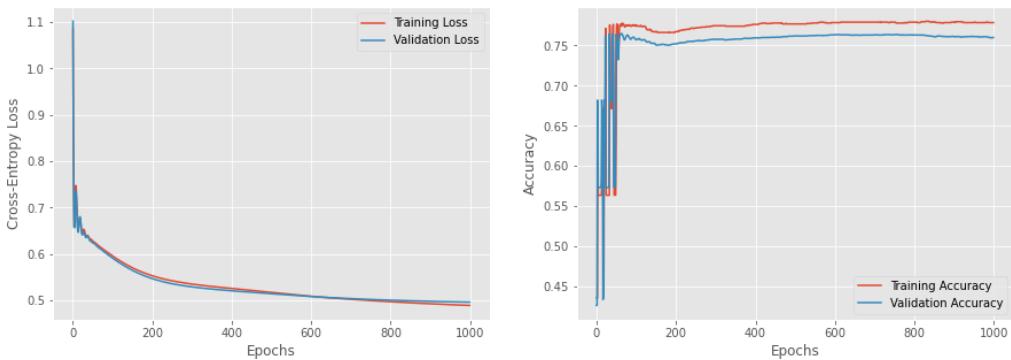


Figure 4.2: GCN Loss- and Accuracy Plots

The confusion matrices and the final accuracies are shown in tables 4.2 & 4.3. GCNs are designed to be used in a transductive setting and the model cannot be applied to new and unseen graphs. In this setting 30% of the dataset are used for training and 70% of the data is used for validation. This is done by masking the nodes in the graph which are part of the validations dataset. The masked nodes

<sup>1</sup>Website Gregory Gundersen:  
<https://gregorygundersen.com/blog/2020/02/09/log-sum-exp/>

Predicted Label	Neutral or Dissatisfied	Satisfied
Neutral or Dissatisfied	776	232
Satisfied	164	616
Accuracy	77.85%	

Table 4.2: Confusion Matrix Training Data GCN

Predicted Label	Neutral or Dissatisfied	Satisfied
Neutral or Dissatisfied	1'828	587
Satisfied	424	1'372
Accuracy	76.00%	

Table 4.3: Confusion Matrix Validation Data GCN

are considered in the neighborhood function  $\mathcal{N}(v)$ , they are just not considered as target nodes for learning and updating the model parameters. The fact, that GCNs cannot be used in an inductive setting is very limiting. Further, the GCN requires 1'000 epochs to finish training and yields only mediocre results in terms of accuracy and model fit. A reason for this could be, that only a full-batch implementation for GCN was introduced. In addition, GCNs always consider the entire neighborhood set. GraphSage for comparison is specifically designed with mini-batch training and neighborhood sampling in mind. The results for GraphSage are presented in the following section.

### 4.2.2 GraphSage

For GraphSage the exact same data input is used as for the GCN. The GraphSage model includes 2 convolutional layers with a hidden layer size of 24 and an output layer size of 2. The model is defined using an adaptation of algorithm 4. Specifically, the hidden layer is activated using the ReLU function with subsequent L2-normalization. The output of the second layer is activated using the logsoftmax function. Normalization is skipped for the final output. The training data is split into 80% training and 20% validation using node masking. The loss is calculated using cross-entropy and the model parameters are updated using the Adam optimizer with the learning rate set to 0.002. The GraphSage model employed is thus an adaptation of the algorithm shown in algorithm 3. The model is trained using a mini-batch size of 50 nodes and the neighborhood function  $\mathcal{N}(v)$  randomly samples 10 neighbors at a 2-hop distance from the target node and randomly samples 5 nodes at a 1-hop distance. This corresponds to the steps shown in figure 2.5. To improve the robustness of the model, a dropout rate of  $p = 0.02$  is set. GraphSage is run using the aggregation strategies mean, LSTM, max-pooling, and sum-pooling.

The model for each aggregation strategy is trained using 400 epochs. The training- and validation results using the training graph are presented for every aggregation strategy. In addition, the trained models are applied to a new unseen test graph which also consists of 6'000 randomly sampled nodes. The test graph is created analogues to the training- and validation graph using a separate test feature dataset. The results for all aggregation strategies are presented in the following paragraphs.

### Mean Aggregation

In figure 4.3 the training- and validation losses as well as the accuracies for the mean aggregation model is shown.

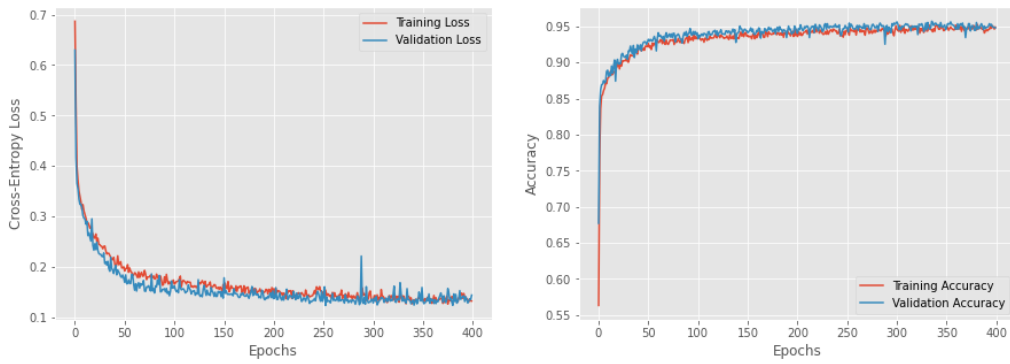


Figure 4.3: Mean Aggregation Loss- and Accuracy Plots

The training accuracy is 94.91% and the validation accuracy is 94.80% after training the model for 400 epochs. The loss- and accuracy plots show a good model fit which remains stable. The model resulted in a test accuracy of 94.08% with the confusion matrix shown in table 4.4:

Predicted Label \ Neutral or Dissatisfied	Neutral or Dissatisfied	Satisfied
Neutral or Dissatisfied	3'278	88
Satisfied	267	2'367
Accuracy	94.08%	

Table 4.4: Test Confusion Matrix Mean Aggregation

### LSTM Aggregation

Figure 4.4 shows the training- and validation loss and the accuracy using LSTM aggregation. The model yields very good results for the training- and validation data sets. The LSTM model is however significantly slower for training purposes compared to the other aggregation methods. This is an inconvenient shortcoming. The training- and validation accuracy after 400 epochs is 95.75% and 95.14% respectively. Here again, it is shown that the training behavior is relatively good. The

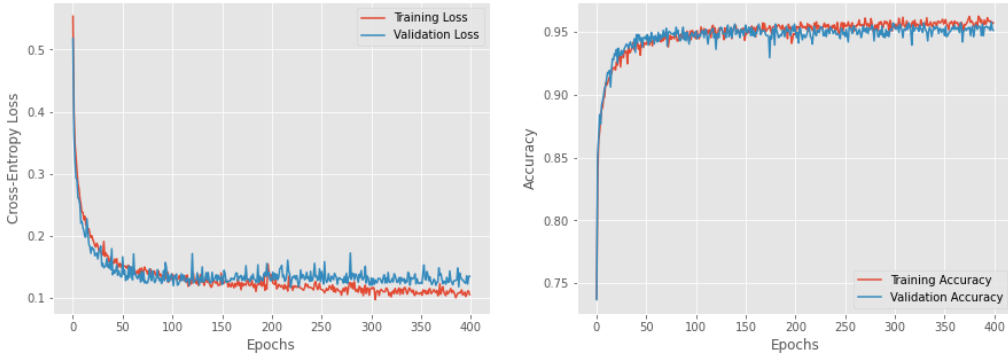


Figure 4.4: LSTM Aggregation Loss- and Accuracy Plots

model is however prone to overfit as shown in figure 4.4. Fortunately, the overfit is small and remains stable. The results for the test graph are shown in table 4.5. The results reveal, that the accuracies of > 95% for the training- and validation datasets do not transfer to the test graph. While this is to be expected, the decrease in accuracy for the test graph is most pronounced for LSTM aggregation. This further indicates, that LSTM aggregation is prone to overfitting.

Predicted Label \ Neutral or Dissatisfied	Neutral or Dissatisfied	Satisfied
Neutral or Dissatisfied	3'288	78
Satisfied	268	2'366
Accuracy	94.23%	

Table 4.5: Test Confusion Matrix LSTM Aggregation

### Sum-Pooling Aggregation

Sum-pooling is added for the reasons outlined in section 2.2.2.2. It is of particular interest to assess, whether sum-pooling can provide some added value compared to the other aggregation strategies. Given the feature data, sum aggregation is unfortunately not injective. For that reason, it is not expected to necessarily dominate the other strategies. Nevertheless, it is of interest to assess, whether sum aggregation is competitive if not superior even in a non-injective setting. The training- and validation results are shown in figure 4.5.

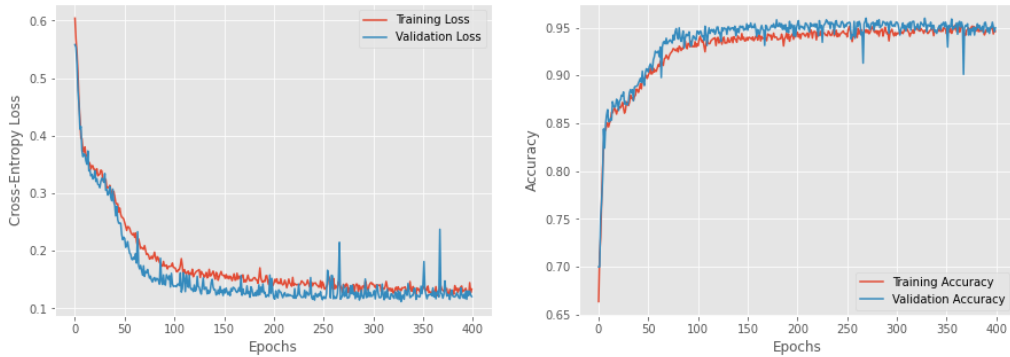


Figure 4.5: Sum-Pooling Aggregation Loss- and Accuracy Plots

The plots show that sum-pooling finishes with a good model fit. The loss curves are however not as smooth compared to the other aggregation strategies. After training for 400 epochs, the training accuracy is at 94.60% and validation accuracy is 94.97%. The results for the test graph are shown in table 4.6. Sum-pooling yields competitive results, it does however not dominate the other aggregation strategies.

Predicted Label \ Neutral or Dissatisfied	Neutral or Dissatisfied	Satisfied
Neutral or Dissatisfied	3'235	131
Satisfied	213	2'421
Accuracy	94.27%	

Table 4.6: Test Confusion Matrix Sum-Pooling

### Max-Pooling Aggregation

The training- and validation loss as well as the accuracies of max-pooling are shown in figure 4.6.

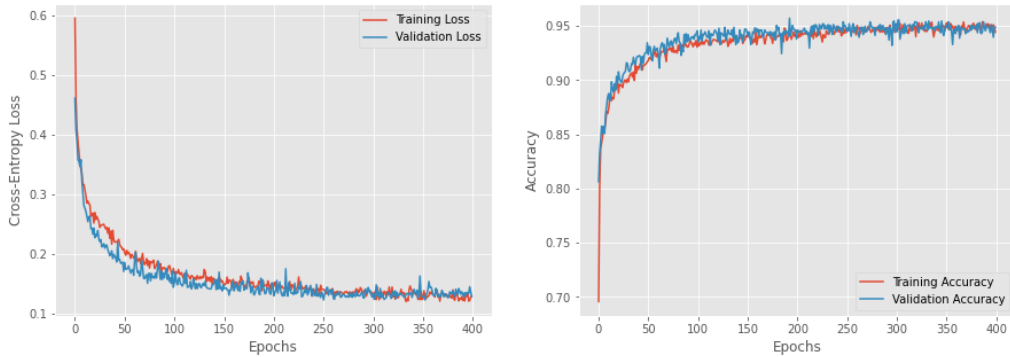


Figure 4.6: Max-Pooling Aggregation Loss- and Accuracy Plots

After 400 epochs, the model arrived at a training accuracy of 94.43% and a validation accuracy of 94.88%. The results for the test graph are shown in table 4.7. Max-

pooling yields the best results and corresponds to the recommended method by Hamilton et al. (2017, p. 9).

Predicted Label \ Neutral or Dissatisfied	Neutral or Dissatisfied	Satisfied
Neutral or Dissatisfied	3'235	131
Satisfied	212	2'422
Accuracy	94.28%	

Table 4.7: Test Confusion Matrix Max-Pooling

### 4.2.3 GraphSage Robustness Simulation

The loss- and accuracy plots using the GraphSage model reveal mostly a relatively good model fit. Repeatedly training the GraphSage models showed, that there is some non-negligible variation in the performance of the trained models. In particular, depending on how the data is randomly split into 80% training data and 20% validation data, the model results could differ significantly. Simulations reveal, that the random assignment of training- and validation data is not the sole culprit for the observed variation in model performance. The dropout rate of 2% employed in the GraphSage model is just as responsible. Simulations show, that if the dropout rate is set to 0, that the model tends to overfit significantly. In this setting, the training accuracy approaches 98% while the validation accuracy stagnates around 92-93%. The trained model accordingly does not translate well to the test graph for which the accuracy is approximately 91%. This training behavior is observed regardless of the random train- and validation data set assignment. For that reason, a dropout rate of 2% is set to avoid this overfitting problem which in turn also yields better test results which are presented in section 4.2.2.

Setting a dropout rate introduces an additional obstacle for training the model. While training, the dropout rate is applied for forward propagating the training data. The validation data is however forward propagated with no dropout. This is the intended mechanism which can be used to prevent overfitting. This however makes the model more sensitive to the random assignment of nodes into training- and validation data. Given the structure present in the graph, some nodes are more difficult to classify than others. If the training data includes more difficult nodes in combination with the dropout rate, the outcome can occur where the validation data has a lower loss and a higher accuracy than the training data. The same can be true in reverse, where an overfit occurs if the training data includes mostly nodes which are more simple to classify than the validation data. Lastly, a good model fit

is also frequently observed as shown in the results presented in the previous section.

Due to this observed variation in model fit and performance, a simulation is performed with 100 experiments. Every experiment makes use of the same training & validation graph and test graph. For every experiment, the training- and validation set is randomly assigned using a 80/20 split. Afterwards, the model is trained using 400 epochs and is then applied to the test graph. The loss and accuracy for the training, validation and test data is collected for every experiment. These experiments are conducted to ensure, that the results shown in section 4.2.2 are representative. The results of the 100 experiments using GraphSage with max-pooling is shown in table 4.8 and figure 4.7.

Metric	Training Set	Validation Set	Test Set
Average Accuracy	94.95%	94.90%	93.79%
	(0.65%)	(0.75%)	(0.41%)
Average Cross-Entropy Loss	0.1276	0.1313	0.1625
	(0.0140)	(0.0170)	(0.0108)

Table 4.8: Simulation Results Max-Pooling

Max-pooling is selected as it corresponds to the recommended aggregation strategy (Hamilton et al. 2017, p. 9). The same simulation using 100 experiments is also performed for sum-pooling. The results are almost identical, where max-pooling is marginally more successful. For the remaining aggregation strategies, only 10 experiments are run due to time considerations as 100 experiments require approximately 15 hours to complete. The required time for the simulation could most definitely be shortened using a graphical processing unit (GPU). Unfortunately, a GPU is not available for conducting the simulations. If available, this would be highly recommended to shorten the required time for completing the simulations. The results using only 10 experiments yields similar results, with test accuracies ranging mostly between 93-94%. The simulation results for mean, LSTM and sum aggregation are shown in appendix A.1. The results shown in section 4.2.2 are therefore representative results, even if admittedly on the more positive side.

## 4.3 Result Comparison

This section compares the results of the three models Node2Vec, GCN and GraphSage. In addition, the graph based ML models are compared to the standard ML models. More precisely, the same standard ML models are used for comparison as for the downstream ML task for GRL shown in section 4.1. For the comparison, the standard ML models consider the same features as inputs as the GNNs. The com-

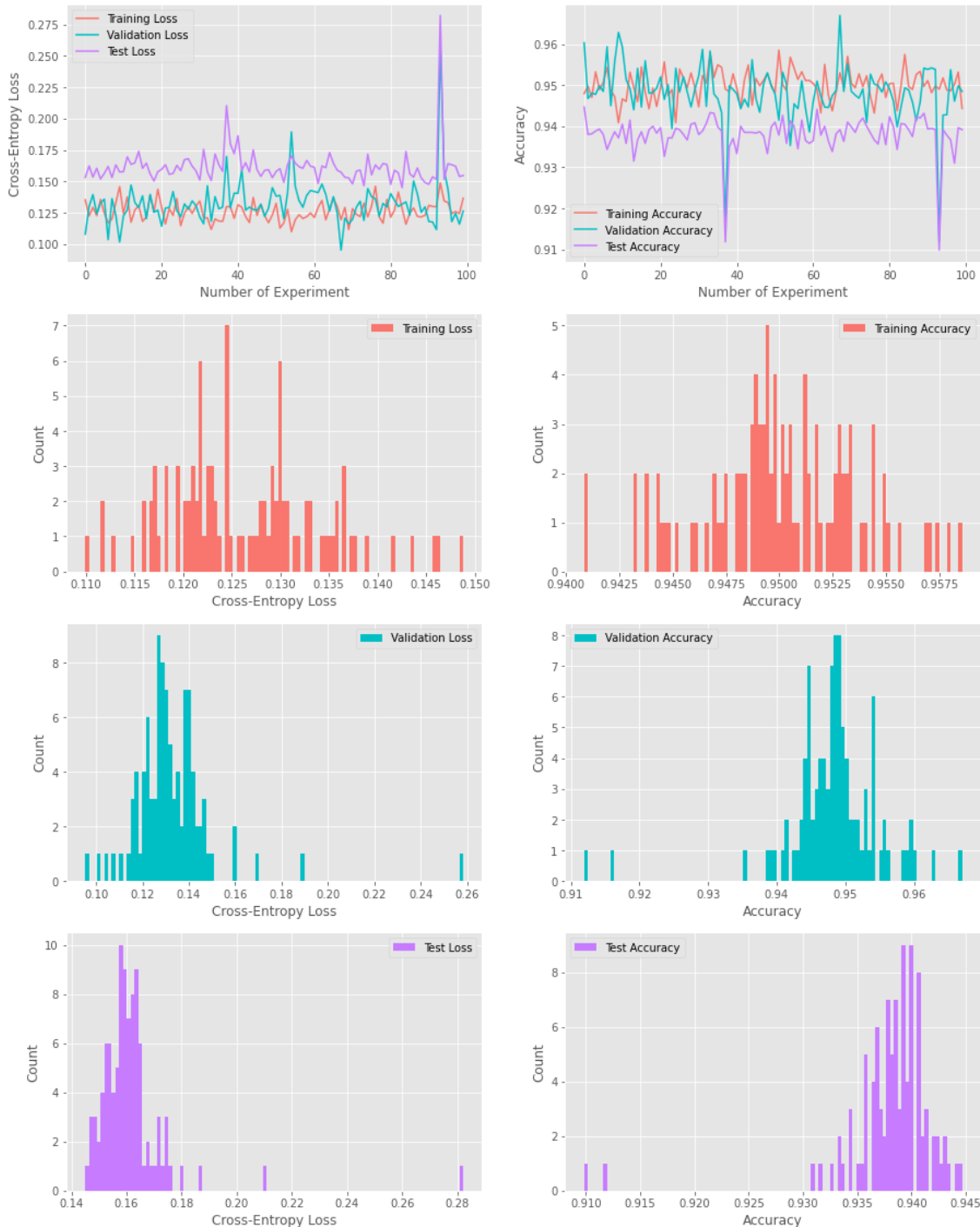


Figure 4.7: Simulation Results Max-Pooling

parison is done to assess to what extent semi-synthetic graphs are useful for GML. This comparison thus provides the key results for answering the research question and assessing the hypotheses stated in section 1.4. The comparison of the results is shown in table 4.9.

Method	Training Accuracy	Validation Accuracy	Test Accuracy
Logistic Regression	87.94%	87.17%	86.77%
Naive Bayes	87.50%	86.17%	85.82%
QDA	70.5%	70.00%	69.23%
AdaBoost	94.06%	92.33%	93.00%
Random Forest	100%	94.42%	94.55%
SVM	94.65%	92.25%	92.73%
ANN	94.86%	95.00%	93.13%
Node2Vec (Logistic Regression)	77.04%	76.16%	57.06%
GCN	77.85%	76.00%	-
GraphSage (Mean Aggregation)	94.91%	94.80%	94.08%
GraphSage (LSTM Aggregation)	95.75%	95.14%	94.23%
GraphSage (Sum-Pooling)	94.60%	94.97%	94.27%
GraphSage (Max-Pooling)	94.43%	94.88%	94.28%

Table 4.9: Result Comparison

The results for the GML models shown in table 4.9 correspond to the results shown in sections 4.1, 4.2.1 and 4.2.2. For GRL (Node2Vec), the results using logistic regression for downstream ML are shown. This method is selected, as it provides the best overall results in terms of accuracy and model simplicity.

The comparison shown in table 4.9 reveals, that GCNs and Node2Vec are not competitive strategies for the US airline passenger dataset. GraphSage is shown to be a serious competitor and is the second best model. The random forest classifier is consistently the best model regardless of the training- and validation data split and the test data. The ANN is the third best model and is only marginally inferior to the GraphSage models. Similarly as for GNNs, it is important to evaluate the model fit of the ANN to draw a more definitive conclusion. The loss- and accuracy plots of the ANN are shown in figure 4.8.

The ANN has an input layer size of 24, a hidden layer size of 15 and an output layer with size 2. The output of the first layer is activated using the ReLU function and the output of the second layer is activated using the softmax function. The loss is calculated using cross-entropy and the model parameters are updated using the Adam optimizer with a learning rate of  $\alpha = 0.002$ . The dropout rate is set to  $p = 0.01$ . Without setting the dropout rate, the ANN is prone to significant overfitting. The presented model settings correspond to the ones which performed best for the ANN. Figure 4.8 shows, that the ANN model starts overfitting after approximately 200 epochs. When comparing the GraphSage training plots with the ANN, the GraphSage model appears to exhibit preferable training behavior on average.

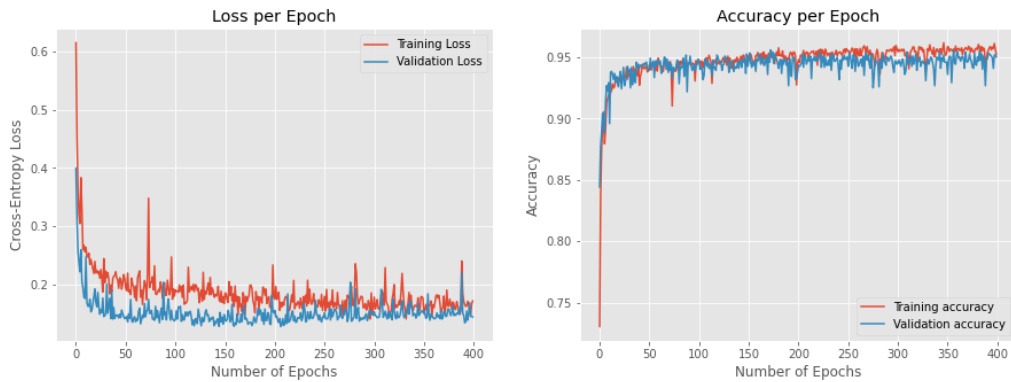


Figure 4.8: ANN Model Fit

AdaBoost and SVM also are shown to yield good results. The test accuracies are however not as competitive compared to the previously mentioned methods. Lastly naive bayes, QDA and logistic regression clearly yield inferior results.

# Chapter 5

## Discussion

The analysis of the data in chapter 3 and the presentation of the ML results in chapter 4 provided a myriad of interesting results. These findings primarily touch following topics and provide the structure for the discussion:

1. Informativeness of semi-synthetic graphs
2. Appropriateness of semi-synthetic graphs for ML
3. GML vs. standard ML

### 5.1 Informativeness of Semi-Synthetic Graphs

The graph generated for the US airline passenger dataset presented in section 3.4 provided interesting results for cluster analysis. The MAG model was successfully used for generating a graph that captured useful neighborhood structures as shown in figure 3.5. Specifically, similar nodes were grouped together based on their similarity given the selected attributes for the MAG model. Especially appealing is that neighborhoods are also consistent within neighborhoods. To illustrate this, one can observe that all nodes are clustered together based on their similarity even within the two main clusters which formed based on the attribute type of travel. This observation is consistent for several additional levels. For instance, nodes form neighborhoods based on age within the cluster of passengers traveling for business purposes. The only attribute for which no significant clusters emerged is gender. The values in the link-affinity matrix for gender were set, so that a connection between the same gender is formed with a probability of 0.6. For observations of the opposite gender, the probability of a connection is 0.4. These probabilities were set based on the assumption, that observations of the same gender are more similar than those of the opposite gender. It is however not assumed, that the passenger experience for women would be significantly different to the one for men. For that

reason, the resulting gender based clusters are only marginally pronounced to the point that no visual interpretations can be made. In addition, one needs to consider the distribution of gender. The attribute is almost perfectly 50/50 split into male and female observations. Assigning more extreme link-affinity probabilities would strongly alter the entire graph. Most likely, the graph would be further split according to gender. In comparison, attributes with more categories can have more extreme values assigned to them. Larger cardinalities have the consequence, that each category affects less nodes. For that reason, one can be less vigilant when assigning link-affinity probabilities for these attributes. Having discussed that, gender did generate some mild clustering within the network. This contributed to the network structure and was successfully exploited using graph machine learning. If gender was not considered for generating the graph, the accuracy of the GraphSage model was slightly decreased.

The graphs shown in figure 3.5 thus provide very useful insights for better understanding the relationships within the data. This is a welcome bi-product of the MAG model and it is surprising to see how informative the resulting graph is for analyzing the data. In fact, it provides vastly superior insights compared to what a standard scatter plot can reveal given the available feature data. For reference, the pairplot of the feature data can be found in appendix C.3. In this regard, the MAG model is very exciting for visually analyzing data.

Applying methods such as Node2Vec further allow for the creation of 2-dimensional node embeddings which can be used to create scatter plots. The scatter plots illustrated in figure 4.1 show the node embeddings of the graph shown in figure 3.5. The scatter plot further helps to solidify the insights gained from the graph. A limitation of the graph for visual interpretation is, that one technically would need to consider the node connections. The large size of the graph however makes it impossible to visually follow the node connections for interpretation. Node2Vec considers the node connections/edges of the network and removes the mentioned limitation for visually interpreting the graph. Figure 4.1 shows, that the visual insights gained from the graph are still valid after considering the node connections. The Node2Vec algorithm is a beautiful dimensionality reduction technique, which successfully reduced the complexity of the graph shown in figures 3.4 & 3.5. In this sense, the MAG in combination with GRL models such as Node2Vec can be used as powerful cluster analysis tools.

## 5.2 Appropriateness of Semi-Synthetic Graphs for Machine Learning

The discussion in the previous section shows, that semi-synthetic graphs themselves can provide valuable visual insights. In this section it is discussed to what extent semi-synthetic graphs are appropriate for GML. The perhaps most instructive evidence is provided by the bank telemarketing dataset presented in section 3.3. GML fails to perform well on the graph generated from this dataset. It is shown, that the attributes chosen for the MAG model are unsuccessful for generating network structures that provided useful additional information which then could be exploited using GML. The bank telemarketing dataset is notoriously difficult due to the unbalanced distribution of the label. The dataset consists of approximately 88% of observations which did not invest in the short-term deposit compared to only 12% of the observations which did invest. For GML and also the standard ML models, it is less optimizing to classify most observations as non-investors. When generating the biased graph shown in figure 3.2, a classification accuracy of  $> 95\%$  was achieved which is a remarkable improvement. As mentioned in section 3.3, the biased graph which includes the label as an attribute cannot be used in a practical setting and is a form of cheating. Nevertheless it shows, that if a network structure can be generated which captures the label well, the problem of unbalanced label data can be overcome. In particular it shows, that the attributes must be capable of generating network structures that are at least in part predictive of the label. Overcoming the problem presented by unbalanced label data is a relevant issue for ML and warrants further research.

The US airline passenger dataset is shown to be well suited for GML. The reasons for its success are in line with the previous discussion regarding the bank telemarketing dataset. The attributes used for the MAG model generated network structures which are in part predictive for the label satisfaction of the US airline passenger dataset. This is shown when looking at the satisfaction plots in figures 3.5 & 4.1.

The graph structure alone yields poor results when looking at the results shown in section 4.1 using Node2Vec. Taking a step back with a more generous perspective, it is nevertheless impressive that an accuracy of approximately 76% could be achieved for the training- and validation dataset which only considered 2-dimensional node embeddings. This however did not translate to the test graph for which the best accuracy was at only approximately 58%. In this sense, the model is only marginally more successful at the classification task than randomly guessing the classification.

GCNs also achieved a classification accuracy of approximately 76%. This result is even worse when comparing it to Node2Vec. The GCN considers the network structure as well as the node features and should therefore be capable of outperforming Node2Vec. The GCN model clearly fails here and has the serious limitation that it cannot be applied in an inductive setting to unseen graphs. The GCN is a breakthrough model as it is one of the first successful GNNs. Nevertheless, it performed poorly for the given datasets and is surpassed in terms of performance by more modern GNN models such as GraphSage.

The final GML model tested is GraphSage. This model yields very good results as shown in section 4.2.2. GraphSage is capable of training models which have a test accuracy of  $> 94\%$ . The aggregation strategies used for the GraphSage model are successful in the order max-pooling  $\geq$  sum-pooling  $>$  LSTM  $>$  mean. This ordering is based on the results presented in section 4.2.2 and is confirmed by the simulation results shown in section 4.2.3 and appendix A.1. When comparing the two main aggregation strategies of interest, max-pooling and sum-pooling, both methods almost yield identical test results. For the results shown in section 4.2.2, max-pooling is only more successful in classifying 1 more passenger as satisfied compared to sum-pooling. The test results are otherwise identical as shown in tables 4.7 & 4.6. The simulation results with 100 experiments for both max-pooling and sum-pooling confirm, that max-pooling yields marginally better results for the test graph with an average accuracy of 93.80% compared to 93.76% for sum-pooling. Sum-pooling is however more consistent, whereas max-pooling has a larger variance regarding the test accuracy. In addition, max-pooling suffered from two large negative test accuracy outliers during the simulation. Sum-pooling also suffered from two negative test accuracy outliers which were however less pronounced. The GraphSage results show, that semi-synthetic graphs can indeed be appropriate for GML.

## 5.3 Graph Machine Learning vs. Standard Machine Learning

The overview in table 4.9 shows, that the results using GraphSage are competitive in comparison to the standard ML models. The results further confirm, that the results using Node2Vec and the GCN are not competitive. GraphSage is proven to be the second best method behind the random forest classifier. The ANN model on average tends to yield marginally inferior test accuracies as presented in the simulation results shown in appendix A.2. In addition, the ANN is more prone to

overfitting as illustrated in figure 4.8. With regard to the other standard ML methods, GraphSage clearly outperformed these models in terms of accuracy.

This shows, that semi-synthetic graphs can be used for GML in a competitive setting. The accuracy improvements one would hope for considering the rather tedious and difficult graph generation procedure is however not achieved. As shown in table 4.9, a simpler models such as the random forest classifier consistently outperforms the GraphSage model. In addition, a simpler standard ANN yields very similar results as GraphSage. In ML the principle of Occam’s razor is often referred to for choosing appropriate models. Following this principle, simpler models are preferred if they yield similar/identical results compared to more complex methods. GraphSage in combination with the semi-synthetic graphs, is most definitely the most complex model shown in table 4.9. For that reason, certainly the random forest classifier is preferred as it yields better accuracies and is a more simple model compared to GraphSage. In addition, one could argue that the ANN, SVM, and AdaBoost are preferential to the GraphSage model as well. These models are simpler with only marginally inferior results. For the evaluation one needs to also consider the context of the classification task. In a medical context, accuracies are of utmost importance where one is willing to use more complex methods to receive marginal accuracy improvements. For the purpose of gaining customer insights, the consequences for having marginally higher- or lower accuracies are less severe. In such a setting, the principle of Occam’s razor can be more fully embraced which is why the ANN, SVM, and AdaBoost might be preferred as they are simpler and more practical for the application in a real world setting. This is a subjective assessment and depending on the context, it might differ. Nevertheless, GraphSage yields the second best accuracies and remains a competitive model.

Last but not least, the comparison of real network properties and the MAG must be discussed as indicated in section 3.4. As shown, the properties of the graph generated from the US airline passenger dataset is not in line with the properties of real networks. At first glance, this might not appear to be of importance. The results presented in chapter 4 however show, that GML was competitive but not superior to standard ML models. The network structure appears to only provide a marginal improvement for the GML models. A reason for this limited success could be, that the vertex degrees are too large. This for instance has the consequence, that the GraphSage model has the same network structure at every layer. According to the model specifications, the GraphSage model samples 10 nodes at the 2-hop distance and 5 nodes at the 1-hop distance. Given, that the degree distribution shown in figure 3.6 starts at 263, the GraphSage model will always sample exactly

10 and 5 nodes respectively. In this setting, only the feature data and the general neighborhood of the nodes can be considered. Specific network structures within the neighborhoods can however not be exploited. This points to a serious limitation of the generated MAG and might be a reason why GraphSage did not perform better. A similar observation is also made for the GCN. This model always has to consider the entire graph Laplacian. Given the large starting value of the degree distribution, this can become a challenging task. While, the model may be able to differentiate general neighborhoods, recognizing more local neighborhoods could prove to be excessively challenging. This is an area which should be investigated for future research.

# Chapter 6

## Conclusion and Outlook

This chapter includes the conclusion and provides an outlook for future research.

### 6.1 Conclusion

The aim of this thesis was to assess to what extent semi-synthetic graphs are useful for gaining customer insights using GML. This aim corresponds to the research question stated in section 1.4. The results for answering this question are mixed and are based on the data presented in chapter 3, the results of chapter 4, and the discussion in chapter 5.

GML on the network created from the bank telemarketing dataset fails to overcome the problem of unbalanced labels. It however yields similar results in terms of accuracy as the standard ML models. In addition it is shown, that if a network structure can be created which corresponds to the label, that the problem of unbalanced label data could be overcome.

GraphSage performs well for the US airline passenger dataset and is second only to the random forest classifier in terms of accuracy. As discussed, following the principle of Occam’s razor, the good results for the GraphSage model must be taken with a grain of salt. For the purpose of gaining customer insights, simpler models such as ANNs, SVMs, and AdaBoost provide only marginally inferior results and are more practical and thus preferable for this setting. Given similar results for more sensitive applications in fields such as medicine, the GraphSage model could be preferred as even marginal performance improvements can be of utmost importance. In short, the GraphSage yields competitive results in terms of accuracy, the results are however not superior enough to necessarily warrant the complex graph generation process and model complexity of GraphSage. Lastly, the GCN and Node2Vec are not successful for the given classification task. For that reason, more recent GML

models should be tested and/or new models should be developed to expand the possibilities of GML.

The perhaps most interesting result is provided by the US airline passenger graph plots shown in figure 3.5. The MAG model successfully generated neighborhoods within the graph, where the nodes are grouped according to their similarity which respects the similarities between all attributes. This observation is further confirmed by the scatterplots shown in figure 4.1. The graphs and the scatterplots make it possible to visually interpret the relationships within the data. Standard scatterplots using the feature data do not allow for the generation of such insightful graphs/plots.

To summarize and provide an answer to the research question, it is shown that yes, semi-synthetic graphs can be useful for GML in a classification setting. The GML models are shown to be competitive and could potentially even provide a solution for overcoming the difficulties associated with unbalanced label data. This however requires the availability of a graph with a structure which corresponds to the label. The usefulness of semi-synthetic graphs are limited by the complexity associated with generating graphs and the general complexity of the GML models. In addition, the network properties of the MAG is a limiting factor for the GML models. The graph based models further fail to outperform the standard ML models and are ranked anywhere between the second to fifth best model depending on how one weights the trade-off between model complexity and accuracy. Based on this, the hypotheses presented in section 1.4 can be answered as follows:

**H1:** Graph machine learning models using semi-synthetic graphs fail to outperform standard machine learning modelss. This hypothesis is thus rejected.

**H2:** Graph machine learning is shown to be a competitive strategy with competitive results in line with the results shown for the standard machine learning models. This hypothesis is not rejected.

## 6.2 Outlook

The discussion in chapter 5 and the conclusion in section 6.1 provides interesting topics for future research. These topics include graph generation, cluster analysis on graphs, and GML models and are presented in the following paragraphs.

### Graph Generation

Creating semi-synthetic graphs using the MAG model is shown to be a viable approach. The graph is however sensitive to attribute selection and setting appropriate link-affinity probabilities. A first step for resolving this issue was introduced by Kim & Leskovec (2011) as a follow up to their MAG model. In this paper they propose a reverse model, in which given a real graph, the attributes and the link-affinity probabilities are estimated such that the attributes and link-affinity probabilities generate the observed real graph. This is however only a partial solution to the task given for this master’s thesis. The estimated attributes do not correspond to real attributes/features. In this model, the attributes are estimated to fit the graph. An interesting topic for future research would be to develop a model that generates a semi-synthetic graph based on real attributes which at the same time optimizes the link-affinity probabilities such that the resulting graph adheres to real network properties. Perhaps these more realistic graph properties can improve the performance for GML. This is an area worth consideration as especially the degree distribution and centrality measures shown in figure 3.6 force GML models to consider a large number of neighbors. In addition even when sampling, the neighborhood is bound to always have the same size given the range of the degree distribution shown in figure 3.6. This is a potentially serious limiting factor for GML, as it makes it more difficult to distinguish between more local structures within the graph.

### Cluster Analysis on Graphs

The graph plots shown in figure 3.5 reveal, that MAGs can be excellent tools for visualizing data. The amount of useful information provided for interpreting the data is a welcome and unexpected result. For understanding the relationships between the attribute data and the label, the graph plots yielded the most useful information for identifying relationships within the data. An interesting topic for future research could be to assess how common clustering models such as k-means, fuzzy clustering or CLIQUE could be used for analyzing graphs. Perhaps better and more graph centric models could be developed. An excellent overview of existing graph clustering models is provided by Zhou et al. (2020). Their article can be used as an initial reference point for identifying new applications of existing graph clustering methods or for developing new models.

### Graph Machine Learning Models

GCNs and GraphSage were selected for this master’s thesis as they are probably the two most well-known GNNs. There are however newer and more sophisticated models such as graph attention networks (GATs) (Veličković et al. 2018) or graph isomorphism networks (GINs) (Xu et al. 2019).

GAT models have the ability of identifying more- or less important neighbors in the graph. This is a useful ability and has been shown to improve performance in some cases. This ability is unfortunately most likely limited by the very large number of vertex degrees present in the US airline passenger graph as shown in figure 3.6. For that reason, more realistic graphs with smaller number of degrees should be generated as discussed in section 5.3.

GIN models are very well suited for distinguishing structures within the graph. The authors Xu et al. (2019) present the general GIN framework which can accept any type of features as inputs whilst ensuring that the aggregation function is injective. Given the injective aggregation strategy, it is shown that the GIN can be as powerful at distinguishing graph structures as the Weisfeiler-Lehman graph isomorphism test (Weisfeiler & Lehman 1968). Again, for such a model to work best, the number of degrees would most likely need to be smaller than currently present in the graph of the US airline passenger dataset. Given the large number of degrees, the neighborhoods of every node are currently of the same size when using the sampling strategy outlined for the GraphSage model.

Given a more realistic graph with a smaller number of degrees, it would be interesting to develop and assess, whether a new model which includes the attention mechanism of the GAT and the isomorphic capabilities of the GIN could be of use. This new model could for instance then be tested on well understood benchmark graphs such as Cora (McCallum et al. 2000) or Citeseer (Giles et al. 1998).

# References

- Abadi, M., Agarwal, A., Barham, P., Brevdo, E., Chen, Z., Citro, C., Corrado, G. S., Davis, A., Dean, J., Devin, M. et al. (2016), ‘Tensorflow: Large-scale machine learning on heterogeneous distributed systems’, *arXiv preprint arXiv:1603.04467*
- URL: <https://arxiv.org/abs/1603.04467>
- Ahmed, A., Shervashidze, N., Narayanamurthy, S., Josifovski, V. & Smola, A. J. (2013), Distributed large-scale natural graph factorization, in ‘Proceedings of the 22nd international conference on World Wide Web’, pp. 37–48.
- URL: <https://doi.org/10.1145/2488388.2488393>
- Alphabet (2021), ‘Alphabet investor relations’. (accessed: 04.05.2021).
- URL: <https://abc.xyz/investor/>
- AlphaFold (2020), ‘Alphafold: a solution to a 50-year-old grand challenge in biology’. (accessed: 05.05.2021).
- URL: <https://deepmind.com/blog/article/alphafold-a-solution-to-a-50-year-old-grand-challenge-in-biology>
- Artisan’s Asylum (2020), ‘Intro to machine learning’. (accessed: 24.06.2021).
- URL: <https://artisansasylum.com/classes/intro-to-machine-learning-2/>
- Barabási, A.-L. & Albert, R. (1999), ‘Emergence of scaling in random networks’, *science* **286**(5439), 509–512.
- URL: <https://doi.org/10.1126/science.286.5439.509>
- Breiman, L. (2001), ‘Random forests’, *Machine learning* **45**(1), 5–32.
- URL: <https://doi.org/10.1023/A:1010933404324>
- Bridle, J. S. (1990a), Probabilistic interpretation of feedforward classification network outputs, with relationships to statistical pattern recognition, in ‘Neurocomputing’, Springer, pp. 227–236.
- URL: [https://doi.org/10.1007/978-3-642-76153-9\\_28](https://doi.org/10.1007/978-3-642-76153-9_28)

- Bridle, J. S. (1990b), Training stochastic model recognition algorithms as networks can lead to maximum mutual information estimation of parameters, in ‘Proceedings of the second conference of Advances in neural information processing systems (NIPS 1989)’, pp. 211–217.
- URL:** <https://papers.nips.cc/paper/1989/file/0336dcbab05b9d5ad24f4333c7658a0e-Paper.pdf>
- Chang, C.-C. & Lin, C.-J. (2011), ‘Libsvm: a library for support vector machines’, *ACM transactions on intelligent systems and technology (TIST)* **2**(3), 1–27.
- URL:** <https://doi.org/10.1145/1961189.1961199>
- Cohen, E. (2021), ‘Node2vec’, <https://github.com/eliorc/node2vec.git>.
- Cramer, J. S. (2002), ‘The origins of logistic regression’.
- URL:** <http://dx.doi.org/10.2139/ssrn.360300>
- da Costa-Luis, C., Larroque, S., Altendorf, K., Mary, H., Korobov, M., Yorav-Raphael, N. et al. (2021), ‘tqdm: A fast, extensible progress bar for python and cli’, *Zenodo. Apr.*
- URL:** <https://doi.org/10.5281/zenodo.595120>
- Dubois, Y. (2019), ‘Interpretation of symmetric normalised graph adjacency matrix?’, Mathematics Stack Exchange.
- URL:** <https://math.stackexchange.com/q/3284214>
- Erdős, P. & Rényi, A. (1959), ‘On random graphs 1’, *Publicationes Mathematicae* **6**, 290–297.
- URL:** <https://snap.stanford.edu/class/cs224w-readings/erdos59random.pdf>
- Euler, L. (1736), ‘Solutio problematis ad geometriam situs pertinentis’, *Commentarii academiae scientiarum Petropolitanae* **8**, 128–140.
- Facebook (2021), ‘Facebook investor relations’. (accessed: 04.05.2021).
- URL:** <https://investor.fb.com/investor-events/default.aspx>
- Frauenhofer Institut (2021), ‘Fame ai and machine learning’. (accessed: 24.06.2021).
- URL:** <https://www.fokus.fraunhofer.de/en/fame/workingareas/ai>
- Freund, Y. & Schapire, R. E. (1997), ‘A decision-theoretic generalization of on-line learning and an application to boosting’, *Journal of computer and system sciences* **55**(1), 119–139.
- URL:** <https://doi.org/10.1006/jcss.1997.1504>

- Giles, C. L., Bollacker, K. D. & Lawrence, S. (1998), Citeseer: An automatic citation indexing system, *in* ‘Proceedings of the third ACM conference on Digital libraries’, pp. 89–98.  
**URL:** <https://dl.acm.org/doi/pdf/10.1145/276675.276685>
- Grover, A. & Leskovec, J. (2016), node2vec: Scalable feature learning for networks, *in* ‘Proceedings of the 22nd ACM SIGKDD international conference on Knowledge discovery and data mining’, pp. 855–864.  
**URL:** <https://doi.org/10.1145/2939672.2939754>
- Gundersen, G. (2020), ‘The log-sum-exp trick’, <https://gregorygundersen.com/blog/2020/02/09/log-sum-exp/>.
- Hagberg, A., Swart, P. & S Chult, D. (2008), Exploring network structure, dynamics, and function using networkx, Technical report, Los Alamos National Lab.(LANL), Los Alamos, NM (United States).  
**URL:** <https://www.osti.gov/biblio/960616>
- Hamilton, W. L., Ying, R. & Leskovec, J. (2017), Inductive representation learning on large graphs, *in* ‘Proceedings of the 31st International Conference on Neural Information Processing Systems’, NIPS’17, Curran Associates Inc., Red Hook, NY, USA, p. 1025–1035.  
**URL:** <https://dl.acm.org/doi/abs/10.5555/3294771.3294869>
- Harris, C. R., Millman, K. J., van der Walt, S. J., Gommers, R., Virtanen, P., Cournapeau, D., Wieser, E., Taylor, J., Berg, S., Smith, N. J., Kern, R., Picus, M., Hoyer, S., van Kerkwijk, M. H., Brett, M., Haldane, A., del Río, J. F., Wiebe, M., Peterson, P., Gérard-Marchant, P., Sheppard, K., Reddy, T., Weckesser, W., Abbasi, H., Gohlke, C. & Oliphant, T. E. (2020), ‘Array programming with NumPy’, *Nature* **585**(7825), 357–362.  
**URL:** <https://doi.org/10.1038/s41586-020-2649-2>
- Hastie, T., Rosset, S., Zhu, J. & Zou, H. (2009), ‘Multi-class adaboost’, *Statistics and its Interface* **2**(3), 349–360.  
**URL:** <https://dx.doi.org/10.4310/SII.2009.v2.n3.a8>
- Hochreiter, S. & Schmidhuber, J. (1997), ‘Long short-term memory’, *Neural computation* **9**(8), 1735–1780.  
**URL:** <https://doi.org/10.1162/neco.1997.9.8.1735>
- Hunter, J. D. (2007), ‘Matplotlib: A 2d graphics environment’, *Computing in Science & Engineering* **9**(3), 90–95.  
**URL:** <https://www.doi.org/10.1109/MCSE.2007.55>

- KAGGLE Inc., T. K. (2020), ‘2015 north america airport satisfaction survey’.  
**URL:** <https://www.kaggle.com/teejmahal20/airline-passenger-satisfaction>
- Katz, L. (1953), ‘A new status index derived from sociometric analysis’, *Psychometrika* **18**(1), 39–43.  
**URL:** <https://doi.org/10.1007/BF02289026>
- KDD (2020), ‘Stochastic training of gnn for node classification on large graphs’.  
**URL:** <https://github.com/dglai/KDD20-Hands-on-Tutorial>
- Kim, M. & Leskovec, J. (2011), ‘Modeling social networks with node attributes using the multiplicative attribute graph model’, *arXiv preprint arXiv:1106.5053* .  
**URL:** <https://arxiv.org/abs/1106.5053>
- Kim, M. & Leskovec, J. (2012), ‘Multiplicative attribute graph model of real-world networks’, *Internet mathematics* **8**(1-2), 113–160.  
**URL:** <https://doi.org/10.1080/15427951.2012.625257>
- Kingma, D. P. & Ba, J. (2015), Adam: A method for stochastic optimization, in ‘Proceedings of the 3rd International Conference on Learning Representations, ICLR 2015, San Diego, CA, USA, May 7-9, 2015’.  
**URL:** <http://arxiv.org/abs/1412.6980>
- Kipf, T. (2016), ‘Graph convolutional networks’. (accessed: 15.05.2021).  
**URL:** <https://tkipf.github.io/graph-convolutional-networks/>
- Kipf, T. N. & Welling, M. (2016), ‘Semi-supervised classification with graph convolutional networks’, *arXiv preprint arXiv:1609.02907* .  
**URL:** <https://arxiv.org/abs/1609.02907>
- Krizhevsky, A., Sutskever, I. & Hinton, G. E. (2012), ‘Imagenet classification with deep convolutional neural networks’, *Advances in neural information processing systems* **25**, 1097–1105.  
**URL:** <https://papers.nips.cc/paper/2012/file/c399862d3b9d6b76c8436e924a68c45b-Paper.pdf>
- Landau, E. (1895), ‘Zur relativen wertbemessung der turnierresultate’, *Deutsches Wochenschach* **11**, 366–369.
- Leskovec, J. (2021), ‘Cs224w lecture at stanford’. (accessed: 15.05.2021).  
**URL:** <http://web.stanford.edu/class/cs224w/>
- Leskovec, J., Chakrabarti, D., Kleinberg, J., Faloutsos, C. & Ghahramani, Z. (2010), ‘Kronecker graphs: an approach to modeling networks.’, *Journal of Machine*

- Learning Research* **11**(2).
- URL:** <https://www.jmlr.org/papers/volume11/leskovec10a/leskovec10a.pdf>
- Li, Y., Vinyals, O., Dyer, C., Pascanu, R. & Battaglia, P. (2018), ‘Learning deep generative models of graphs’, *arXiv preprint arXiv:1803.03324*.
- URL:** <https://arxiv.org/abs/1803.03324>
- McCallum, A. K., Nigam, K., Rennie, J. & Seymore, K. (2000), ‘Automating the construction of internet portals with machine learning’, *Information Retrieval* **3**(2), 127–163.
- URL:** <https://doi.org/10.1023/A:1009953814988>
- McCulloch, W. S. & Pitts, W. (1943), ‘A logical calculus of the ideas immanent in nervous activity’, *The bulletin of mathematical biophysics* **5**(4), 115–133.
- URL:** <https://doi.org/10.1007/BF02478259>
- McKinney, W. et al. (2010), Data structures for statistical computing in python, in ‘Proceedings of the 9th Python in Science Conference’, Vol. 445, Austin, TX, pp. 51–56.
- URL:** <http://conference.scipy.org/proceedings/scipy2010/pdfs/mckinney.pdf>
- Mikolov, T., Chen, K., Corrado, G. & Dean, J. (2013a), ‘Efficient estimation of word representations in vector space’, *arXiv preprint arXiv:1301.3781*.
- URL:** <https://arxiv.org/abs/1301.3781>
- Mikolov, T., Sutskever, I., Chen, K., Corrado, G. & Dean, J. (2013b), ‘Distributed representations of words and phrases and their compositionality’, *arXiv preprint arXiv:1310.4546*.
- URL:** <https://arxiv.org/abs/1310.4546>
- Moro, S., Cortez, P. & Rita, P. (2014), ‘A data-driven approach to predict the success of bank telemarketing’, *Decision Support Systems* **62**, 22–31.
- URL:** <https://doi.org/10.1016/j.dss.2014.03.001>
- Moro, S., Laureano, R. & Cortez, P. (2011), ‘Using data mining for bank direct marketing: An application of the crisp-dm methodology’.
- URL:** <http://hdl.handle.net/1822/14838>
- Nair, V. & Hinton, G. E. (2010), Rectified linear units improve restricted boltzmann machines, in ‘Proceedings of the 27th International Conference on International Conference on Machine Learning (ICML 2010)’.
- URL:** <https://dl.acm.org/doi/10.5555/3104322.3104425>
- Newman, M. (2010), *Networks: An Introduction*, Oxford University Press, Inc.

- Newman, M. E., Barabási, A.-L. E. & Watts, D. J. (2006), *The structure and dynamics of networks.*, Princeton university press.
- OECD (2017), ‘G20/oecd infe report on adult financial literacy in g20 countries’. (accessed: 10.04.2021).  
**URL:** <https://www.oecd.org/finance/g20-oecd-infe-report-adult-financial-literacy-in-g20-countries.htm>
- Page, L., Brin, S., Motwani, R. & Winograd, T. (1999), The pagerank citation ranking: Bringing order to the web., Technical report, Stanford InfoLab.  
**URL:** <http://ilpubs.stanford.edu:8090/422/>
- Paszke, A., Gross, S., Massa, F., Lerer, A., Bradbury, J., Chanan, G., Killeen, T., Lin, Z., Gimelshein, N., Antiga, L. et al. (2019), ‘Pytorch: An imperative style, high-performance deep learning library’, *arXiv preprint arXiv:1912.01703* .  
**URL:** <https://arxiv.org/abs/1912.01703>
- Pedregosa, F., Varoquaux, G., Gramfort, A., Michel, V., Thirion, B., Grisel, O., Blondel, M., Prettenhofer, P., Weiss, R., Dubourg, V. et al. (2011), ‘Scikit-learn: Machine learning in python’, *the Journal of machine Learning research* **12**, 2825–2830.  
**URL:** <https://www.jmlr.org/papers/volume12/pedregosa11a/pedregosa11a.pdf>
- Perozzi, B., Al-Rfou, R. & Skiena, S. (2014), Deepwalk: Online learning of social representations, in ‘Proceedings of the 20th ACM SIGKDD international conference on Knowledge discovery and data mining’, pp. 701–710.  
**URL:** <https://doi.org/10.1145/2623330.2623732>
- Platt, J. et al. (1999), ‘Probabilistic outputs for support vector machines and comparisons to regularized likelihood methods’, *Advances in large margin classifiers* **10**(3), 61–74.  
**URL:** <http://citeseer.ist.psu.edu/viewdoc/summary?doi=10.1.1.41.1639>
- Power, J. (2015), ‘2015 north america airport satisfaction survey’.  
**URL:** <https://www.jdpower.com/business/press-releases/2015-north-america-airport-satisfaction-study>
- Schweitzer, F., Fagiolo, G., Sornette, D., Vega-Redondo, F., Vespignani, A. & White, D. R. (2009), ‘Economic networks: The new challenges’, *science* **325**(5939), 422–425.  
**URL:** <https://doi.org/10.1126/science.1173644>

- Seabold, S. & Perktold, J. (2010), Statsmodels: Econometric and statistical modeling with python, in ‘Proceedings of the 9th Python in Science Conference’, Vol. 57, Austin, TX, p. 61.  
**URL:** <http://conference.scipy.org/proceedings/scipy2010/pdfs/seabold.pdf>
- Senior, A. W., Evans, R., Jumper, J., Kirkpatrick, J., Sifre, L., Green, T., Qin, C., Žídek, A., Nelson, A. W., Bridgland, A. et al. (2020), ‘Improved protein structure prediction using potentials from deep learning’, *Nature* **577**(7792), 706–710.  
**URL:** <https://doi.org/10.1038/s41586-019-1923-7>
- Tang, J., Qu, M., Wang, M., Zhang, M., Yan, J. & Mei, Q. (2015), Line: Large-scale information network embedding, in ‘Proceedings of the 24th international conference on world wide web’, pp. 1067–1077.  
**URL:** <https://doi.org/10.1145/2736277.2741093>
- Tharwat, A. (2016), ‘Linear vs. quadratic discriminant analysis classifier: a tutorial’, *International Journal of Applied Pattern Recognition* **3**(2), 145–180.  
**URL:** <https://doi.org/10.1504%2FIJAPR.2016.079050>
- Van Rossum, G. & Drake, F. L. (2009), *Python 3 Reference Manual*, CreateSpace, Scotts Valley, CA.
- Veličković, P., Cucurull, G., Casanova, A., Romero, A., Lio, P. & Bengio, Y. (2018), Graph attention networks, in ‘Proceedings of the 6th International Conference on Learning Representations, ICLR 2018, Vancouver, BC, Canada, April 30 - Mai 3, 2018’.  
**URL:** <https://arxiv.org/abs/1710.10903>
- Wang, M., Zheng, D., Ye, Z., Gan, Q., Li, M., Song, X., Zhou, J., Ma, C., Yu, L., Gai, Y. et al. (2019), ‘Deep graph library: A graph-centric, highly-performant package for graph neural networks’, *arXiv preprint arXiv:1909.01315* .  
**URL:** <https://arxiv.org/abs/1909.01315>
- Waskom, M. L. (2021), ‘seaborn: statistical data visualization’, *Journal of Open Source Software* **6**(60), 3021.  
**URL:** <https://doi.org/10.21105/joss.03021>
- Watts, D. J. & Strogatz, S. H. (1998), ‘Collective dynamics of ‘small-world’networks’, *nature* **393**(6684), 440–442.  
**URL:** <https://doi.org/10.1038/30918>
- Weisfeiler, B. & Lehman, A. A. (1968), ‘A reduction of a graph to a canonical form and an algebra arising during this reduction’, *Nauchno-Technicheskaya Informatiya* **2**(9), 12–16.

Werbos, P. (1974), ‘Beyond regression:” new tools for prediction and analysis in the behavioral sciences’, *Ph. D. dissertation, Harvard University* .

Xu, K., Hu, W., Leskovec, J. & Jegelka, S. (2019), How powerful are graph neural networks?, *in* ‘Proceedings of the 7th International Conference on Learning Representation, ICLR 2019, New Orleans, LA, USA, May 6-9, 2019’.

**URL:** <https://arxiv.org/abs/1810.00826>

You, J., Ying, R., Ren, X., Hamilton, W. & Leskovec, J. (2018), Graphrnn: Generating realistic graphs with deep auto-regressive models, *in* ‘International Conference on Machine Learning’, PMLR, pp. 5708–5717.

**URL:** <http://proceedings.mlr.press/v80/you18a.html>

You, J., Ying, Z. & Leskovec, J. (2020), ‘Design space for graph neural networks’, *Advances in Neural Information Processing Systems* **33**.

**URL:** <https://proceedings.neurips.cc/paper/2020/hash/c5c3d4fe6b2cc463c7d7ecba17cc9de7-Abstract.html>

Zhang, H. (2004), The optimality of naive bayes, *in* ‘Proceedings of the 17th International Florida Artificial Intelligence Research Society Conference, FLAIRS 2004, Miami Beach, FL, USA, May 12-14, 2004’.

**URL:** <https://www.aaai.org/Papers/FLAIRS/2004/Flairs04-097.pdf>

Zhou, J., Cui, G., Hu, S., Zhang, Z., Yang, C., Liu, Z., Wang, L., Li, C. & Sun, M. (2020), ‘Graph neural networks: A review of methods and applications’, *AI Open* **1**, 57–81.

**URL:** <https://doi.org/10.1016/j.aiopen.2021.01.001>

# Appendix A

## Simulation Results

### A.1 GraphSage Simulation Results

The results for the GraphSage simulations referenced in section 4.2.3 are presented in appendix A.1. First, the results for sum-pooling are presented in figure A.1 and table A.1.

Metric	Training Set	Validation Set	Test Set
Average Accuracy	94.63%	94.78%	93.76%
	(0.46%)	(0.60%)	(0.37%)
Average Cross-Entropy Loss	0.1346	0.1346	0.1584
	(0.0109)	(0.0144)	(0.0096)

Table A.1: Simulation Results Sum-Pooling

The results for mean aggregation are presented in figure A.2 and table A.2.

Metric	Training Set	Validation Set	Test Set
Average Accuracy	94.75%	95.00%	93.63%
	(0.59%)	(0.56%)	(0.37%)
Average Cross-Entropy Loss	0.1353	0.1341	0.1665
	(0.0122)	(0.0171)	(0.0099)

Table A.2: Simulation Results Mean Aggregation

The results for LSTM aggregation are lastly presented in figure A.3 and table A.3.

Metric	Training Set	Validation Set	Test Set
Average Accuracy	95.64%	94.62%	93.75%
	(0.20%)	(0.69%)	(0.32%)
Average Cross-Entropy Loss	0.1130	0.1407	0.1630
	(0.0047)	(0.0120)	(0.0084)

Table A.3: Simulation Results LSTM Aggregation



Figure A.1: Simulations Results Sum-Pooling

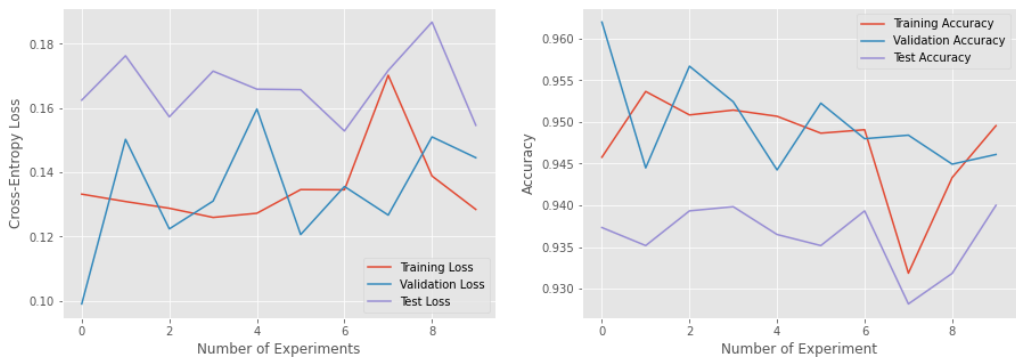


Figure A.2: Simulation Results Mean Aggregation



Figure A.3: Simulation Results LSTM Aggregation

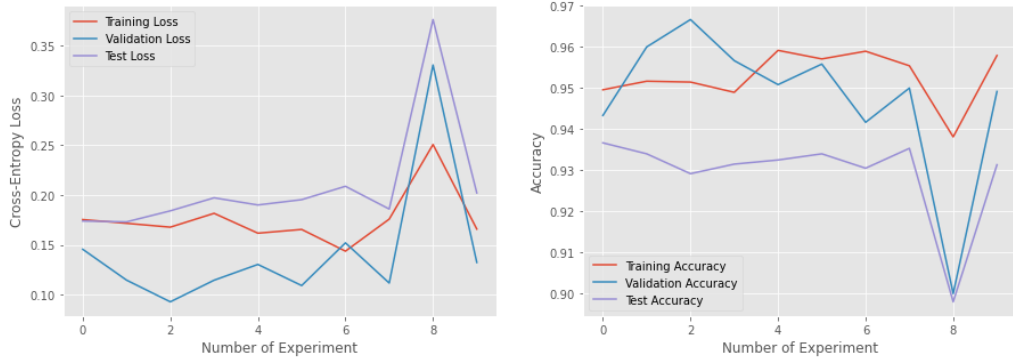


Figure A.4: Simulation Results ANN

## A.2 ANN Simulation Results

Appendix A.1 contains the results for the ANN were simulated using 10 experiments which trained the model for 400 epochs. The results are shown in figure A.4 and table A.4.

Metric	Training Set	Validation Set	Test Set
Average Accuracy	95.28%	94.74%	92.93%
	(0.61%)	(1.73%)	(1.07%)
Average Cross-Entropy Loss	0.1760	0.1433	0.2087
	(0.0268)	(0.0647)	(0.0569)

Table A.4: Simulation Results ANN

# Appendix B

## Auxhiliary Node2Vec Results

### B.1 Node2Vec Results for the Bank Telemarketing Dataset

Appendix B.1 contains the results using Node2Vec for the bank telemarketing dataset are shown in table B.1. For the downstream ML 6-dimensional node embeddings were used.

The models failed to overcome the challenge of unbalanced data for the training- and validation dataset. For that reason, Node2Vec was discarded for further analysis.

### B.2 Node2Vec Results for the US Airline Passenger Dataset

Appendix B.2 contains the results for Node2Vec using 5-dimensional embeddings. Additional experiments with 15-dimensional embeddings further revealed, that generating higher dimensional node embeddings did not improve the accuracy of the downstream ML models. In fact, it decreased the model accuracies. To keep things simple, only the additional results using 5 embeddings are shown in table B.2.

The Node2Vec results which added the feature data to the 2-dimensional node em-

ML Method	Training Accuracy	Validation Accuracy
Logistic Regression	87.64%	89.95%
Support Vector Machine	88.69%	87.62%
ANN	88.00%	89.72%
Random Forest	100%	87.40%
AdaBoost	89.52%	87.18%
QDA	86.06%	84.64%

Table B.1: Node2Vec Classification Results Bank Telemarketing Dataset

ML Method	Training Accuracy	Validation Accuracy
Logistic Regression	56.375%	59.75%
Support Vector Machine	57.52%	55.17%
ANN	57.93%	56.08%
Random Forest	100%	54.08%
AdaBoost	60.54%	53.58%
Naive Bayes	57.52%	55.17%
QDA	57.46%	55.17%

Table B.2: Node2Vec Classification Results with 5-Dimensional Embeddings

ML Method	Training Accuracy	Validation Accuracy	Test Accuracy
Logistic Regression	88.56%	86.00%	87.13%
Support Vector Machine	93.88%	94.08%	83.60%
ANN	96.04%	95.42%	84.50%
Random Forest	100%	93.83%	92.78%
AdaBoost	93.58%	92.50%	83.06%
Naive Bayes	85.88%	87.17%	82.67%
QDA	84.67%	85.08%	76.22%

Table B.3: Node2Vec Classification Results with Feature Data

beddings are presented in table B.3.

# Appendix C

## Various Auxhiliary Results

### C.1 Standard ML Results

Appendix C.1 contains the standard ML results for the bank telemarketing dataset and is shown in table C.1.

### C.2 Deterministic Graph Results

Appendix C.2 contains the results for the deterministically generated MAG presented in section 3.4.2. Figure C.1 and table C.2 show the GraphSage results using max-pooling.

### C.3 Pairplot of US Airline Passenger Dataset

Appendix C.3 contains the pairplot of the feature data of the US airline passenger dataset referenced in section 5.1 is depicted in figure C.2.

ML Method	Training Accuracy	Validation Accuracy
Support Vector Machine	91.54%	88.61%
ANN	90.25%	88.33%
Random Forest	100%	88.75%

Table C.1: Standard ML Results Bank Telemarketing Dataset

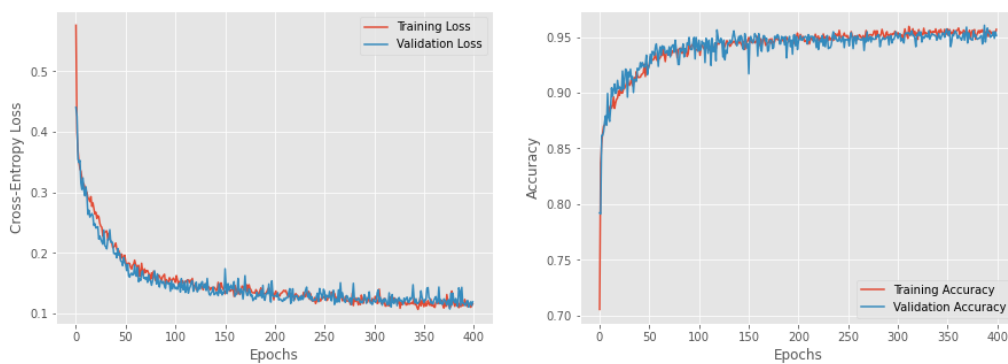


Figure C.1: Max-Pooling Loss- and Accuracy Plots Deterministic MAG

Predicted Label	Neutral or Dissatisfied	Satisfied
Neutral or Dissatisfied	3'167	163
Satisfied	191	2'479
Accuracy	94.10%	

Table C.2: Test Confusion Matrix Deterministic MAG

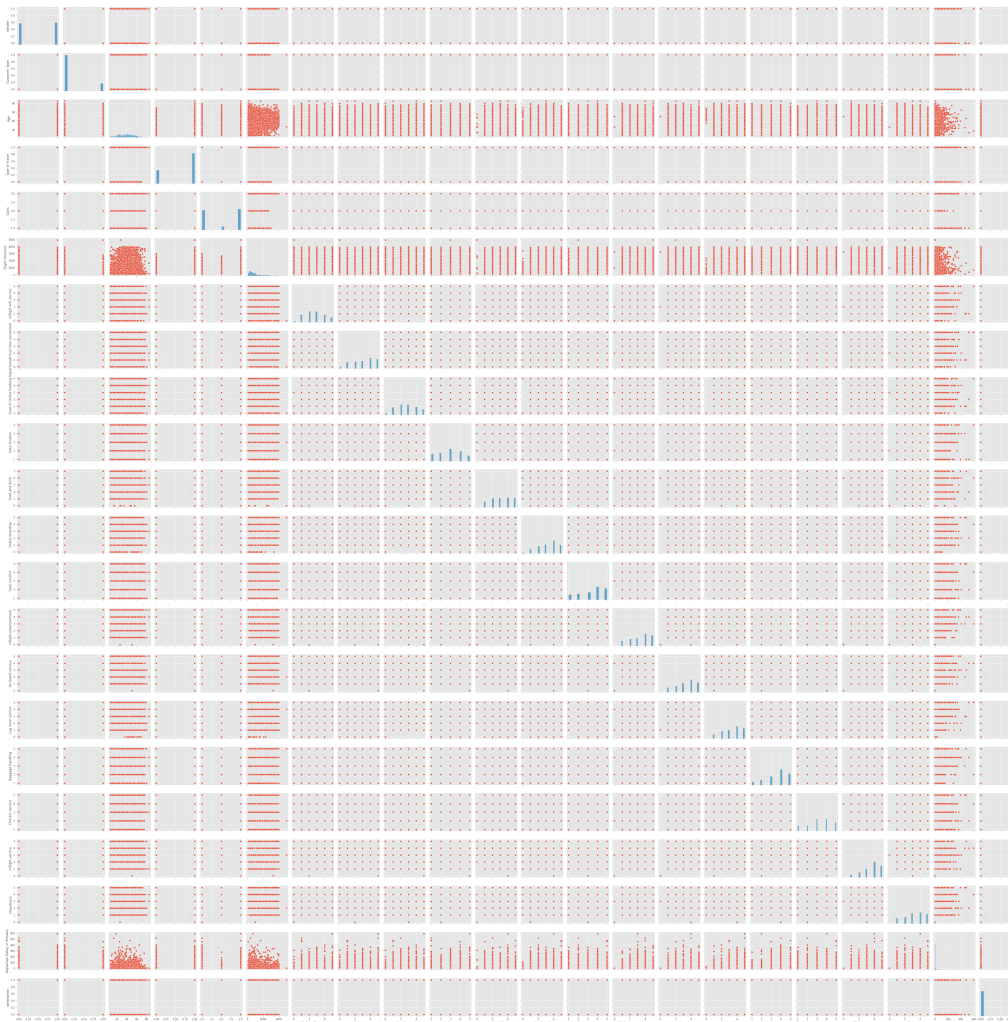


Figure C.2: Pairplot Feature Data US Airline Passenger Dataset

# Declaration

"I hereby declare - that I have written this master's thesis without any help from others and without the use of documents and aids other than those stated in the references, - that I have mentioned all the sources used and that I have cited them correctly according to the established academic citation rules, - that the topic or part of it are not already the object of any work or examination of another course unless explicitly stated,- that I am aware of the consequences of plagiarism at the Faculty of Business and Economics of the University of Basel as stated in the faculty guidelines dated February 22, 2011."

A handwritten signature in black ink, appearing to read "Michael von Siebenthal", is placed over a small grid of dashed lines.

Michael von Siebenthal, Martikel-Nr.: 2015-256-837, Date: July 15, 2021